Neurobiology of Aging 102 (2021) 50–63

Contents lists available at ScienceDirect

Neurobiology of Aging

journal homepage: www.elsevier.com/locate/neuaging.org

Brain tissue properties link cardio-vascular risk factors, mood and cognitive performance in the CoLaus|PsyCoLaus epidemiological cohort

Olga Trofimova[a], Leyla Loued-Khenissi[a], Giulia DiDomenicantonio[a], Antoine Lutti[a], Matthias Kliegel[c], Silvia Stringhini[d,e], Pedro Marques-Vidal[b], Peter Vollenweider[b], Gérard Waeber[b], Martin Preisig[f], Ferath Kherif[a], Bogdan Draganski[a,g,*]

[a] Department of Clinical Neurosciences, Laboratory for Research in Neuroimaging LREN, Centre for Research in Neurosciences, Lausanne University Hospital and University of Lausanne, Lausanne, Switzerland
[b] Department of Medicine, Internal Medicine, Lausanne University Hospital and University of Lausanne, Lausanne, Switzerland
[c] Department of Psychology, University of Geneva, Geneva, Switzerland
[d] Center for Primary Care and Public Health (Unisanté), University of Lausanne, Lausanne, Switzerland
[e] Institute of Social and Preventive Medicine, Lausanne University Hospital, Lausanne, Switzerland
[f] Center for Research in Psychiatric Epidemiology and Psychopathology, Department of Psychiatry, Lausanne University Hospital and University of Lausanne, Lausanne, Switzerland
[g] Neurology Department, Max-Planck-Institute for Human Cognitive and Brain Sciences, Leipzig, Germany

ARTICLE INFO

Article history:
Received 18 September 2020
Revised 31 January 2021
Accepted 4 February 2021
Available online 16 February 2021

Keywords:
Aging
Cardiovascular disease
Cognition
Major depressive disorder
Quantitative magnetic resonance imaging

ABSTRACT

Given the controversy about the impact of modifiable risk factors on mood and cognition in ageing, we sought to investigate the associations between cardio-vascular risk, mental health, cognitive performance and brain anatomy in mid- to old age. We analyzed a set of risk factors together with multi-parameter magnetic resonance imaging (MRI) in the CoLaus|PsyCoLaus cohort ($n > 1200$). Cardio-vascular risk was associated with differences in brain tissue properties – myelin, free tissue water, iron content – and regional brain volumes that we interpret in the context of micro-vascular hypoxic lesions and neurodegeneration. The interaction between clinical subtypes of major depressive disorder and cardio-vascular risk factors showed differential associations with brain structure depending on individuals' lifetime trajectory. There was a negative correlation between melancholic depression, anxiety and MRI markers of myelin and iron content in the hippocampus and anterior cingulate. Verbal memory and verbal fluency performance were positively correlated with left amygdala volumes. The concomitant analysis of brain morphometry and tissue properties allowed for a neuro-biological interpretation of the link between modifiable risk factors and brain health.

1. Introduction

Despite the positive aspects of rising longevity worldwide (Foreman et al., 2018; Kontis et al., 2017), ageing-associated brain disorders such as Alzheimer's disease, vascular dementia, and late-life depression present an increasing burden on older individuals and society. The association between ageing and cognitive decline is modulated by a plenitude of known (e.g. the apolipoprotein APOE*e4 allele) and unknown genetic factors, by environmental (Killin et al., 2016), lifestyle and cardio-vascular risk factors (CVRFs) (Kivipelto et al., 2018), that act across the entire lifespan. Similarly for mood disorders, recent evidence supports the link between late-life depression and cardio-vascular risk in the context of ageing (van den Berg et al., 2019). Much less is known

* Corresponding author at: Bogdan Draganski, Department of Clinical Neurosciences, Laboratory for Research in Neuroimaging LREN, Centre for Research in Neurosciences, Lausanne University Hospital and University of Lausanne, Mont Paisible 16, Lausanne 1011, Switzerland. Tel.: +41 21 314 96 38.
E-mail addresses: bogdan.draganski@gmail.com, bogdan.draganski@chuv.ch (B. Draganski).

0197-4580/$ – see front matter
https://doi.org/10.1016/j.neurobiolaging.2021.02.002

about the neuro-biological mechanisms related to the main effects and interactions between cardio-vascular risk factors, which could explain individuals' affective or cognitive outcomes.

There is strong empirical evidence supporting the impact of CVRFs on cognitive performance in old age (Deckers et al., 2017; Leritz et al., 2011; Marseglia et al., 2019). Already in middle-aged cognitively healthy adults, CVRFs have strong predictive value for future cognitive outcome (Takeda et al., 2017). Studies in older populations confirmed the importance of CVRFs-associated micro-vascular white matter lesions for individuals' cognitive performance (Prins and Scheltens, 2015) that is further modulated by metabolic and inflammatory factors (Wang et al., 2016).

Evidence suggest that the relationship between CVRFs and mood disorders is bidirectional. Large-scale epidemiological studies reported an association between early-life CVRFs and higher risk for late-life depression (Åberg et al., 2012; Baghai et al., 2011), suicidal behavior (Åberg et al., 2014), anxiety and depression symptoms (Jani et al., 2014). At the same time, major depressive disorder (MDD) is viewed as an independent CVRF (Van der Kooy et al., 2007) given its association with increased mortality (Dhar and Barton, 2016; Fiedorowicz, 2014), coronary heart disease (Vaccarino et al., 2020), arterial hypertension, tobacco use, obesity, low physical exercise capacity, and dyslipidemia (Rubin et al., 2010).

The widespread use of computational anatomy methods for analyzing magnetic resonance imaging (MRI) data, helped demonstrating characteristic brain patterns associated either with cognitive decline (Ruan et al., 2016), depression (Geerlings and Gerritsen, 2017; Woelfer et al., 2019) or CVRFs (Cox et al., 2019; Hamer and Batty, 2019). The emergence of large-scale cohorts with brain MRI data acquisition in the general population as exemplified by the UK Biobank (Miller et al., 2016; Sudlow et al., 2015) and Cam-CAN (Shafto et al., 2014), allowed investigating the relationship between CVRFs and brain anatomy in older age. However, the inferences derived from these studies were mostly based on T1-weighted MRI protocols that can result in spurious morphometric findings (Lorio et al., 2016). Advances in quantitative MRI (qMRI) sensitive to iron, myelin and MR-visible water proved the robustness of relaxometry-based measurements against artefactual estimation of regional brain volume or cortical thickness due to MR contrast changes caused by underlying tissue property alterations in brain development (Natu et al., 2019) and ageing (Lorio et al., 2016; Taubert et al., 2020). To date, there were no studies investigating CVRFs-related brain tissue property differences in the context of cognitive and mental health in the general population.

Here, we sought to investigate in a large-scale (n = 1261), population-based sample of adults (BrainLaus cohort age range 45-86 years old from the CoLaus|PsyCoLaus N = 6734), the associations between CVRFs, cognitive performance, and mood, together with their brain anatomy correlates. Our statistical modelling proceeded in multiple stages. Prior to the analyses we ascertained that the BrainLaus cohort was exempt from sampling bias and representative of the parent population-based cohort CoLaus|PsyCoLaus. In the first stage, we identified associations among CVRFs, psychometric and cognitive outcomes. We then extended these analyses with the inclusion of brain measures of tissue property and volume across all regions-of-interest (ROI). Finally, aiming to reduce the dimensionality of our model of multi-contrast MRI and multimodal clinical observations, we analyzed brain volume and tissue microstructure in an informed subset of ROI. Building on our previous work on the effects of age on brain volume, myelin and iron content (Lorio et al., 2016; Taubert et al., 2020), we hypothesized that CVRFs would primarily correlate with brain myelin and tissue water content via micro-vascular hypoxic lesions. We predicted that cognitive performance and mood would be associated with a differential pattern of volume and tissue property differences in specific cortical and subcortical brain structures.

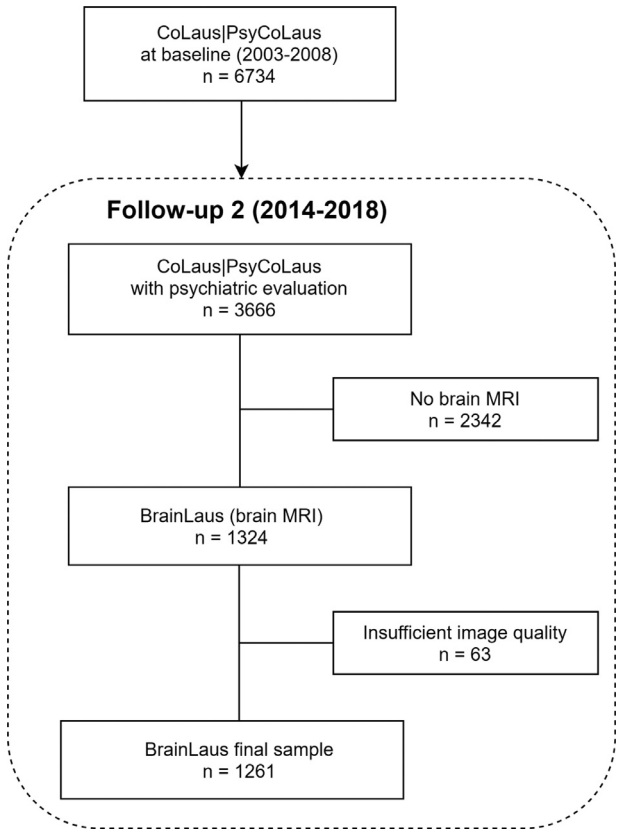

Fig. 1. Timeline of CoLaus|PsyCoLaus and the nested BrainLaus sub-study.

2. Materials and methods

2.1. Participants

Our study sample BrainLaus (https://www.colaus-psycolaus.ch/professionals/brainlaus/) is part of the CoLaus|PsyCoLaus cohort (Firmann et al., 2008; Preisig et al., 2009), a prospective follow-up study designed to determine the associations between CVRFs and mental disorders in the general population. A total of 6734 individuals aged 35 to 75 years were recruited from the civil registry of Lausanne, Switzerland between 2003 and 2006 (baseline) following a random selection procedure. There were two follow-up evaluations, which took place from 2009 to 2013 (first follow-up) and 2014 to 2018 (second follow-up). Among the 3666 people who participated in the second psychiatric follow-up evaluation, 1324 accepted to take part in the brain imaging investigation (BrainLaus). After quantitative MRI data quality assessment (see *2.3 Data quality assessment*) we excluded 63 participants (4.7%), which resulted in 1261 participants included in the analyses (Fig. 1). The CoLaus|PsyCoLaus study and the BrainLaus nested study received approval from the local Ethics Committee and participants signed written informed consent prior to inclusion in the study.

2.2. MRI protocol and data processing

We acquired magnetic resonance images on a 3T whole-body MRI system (Magnetom Prisma, Siemens Medical Systems, Germany), using a 64-channel radio-frequency (RF) receive head coil

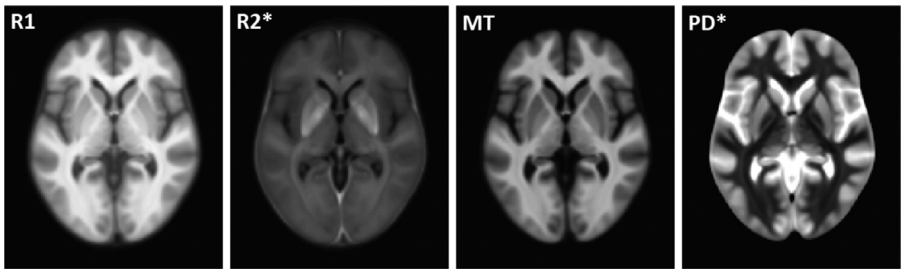

Fig. 2. Group-average anatomical multi-parameter maps R1, R2*, MT, and PD* (n = 1261).

and body coil for transmission. The qMRI protocol included three multi-echo 3D fast low angle shot (FLASH) acquisitions with magnetization transfer-weighted (MTw: TR = 24.5 ms, $\alpha = 6°$), proton density-weighted (PDw: TR = 24.5 ms, $\alpha = 6°$), and T1-weighted (TR = 24.5 ms, $\alpha = 21°$) contrasts at 1 mm isotropic resolution (Draganski et al., 2011; Weiskopf et al., 2013). To correct for the effects of RF transmit field inhomogeneities (Lutti et al., 2014), B1 mapping data was acquired using the 3D EPI spin-echo and stimulated echo method described in (Lutti et al., 2010; Lutti et al., 2012) (4 mm^3 resolution, TE = 39.06 ms, TR = 500 ms). B0-field mapping data was acquired to correct image distortions in the EPI data (2D double-echo FLASH sequence with slice thickness = 2 mm, TR = 1020 ms, TE1/TE2 = 10/12.46 ms, $\alpha = 90°$, BW = 260 Hz/pixel). The total acquisition time was 27 min.

Quantitative MRI maps were calculated from the raw data as described in (Helms et al., 2008a; Helms et al., 2008b) using the VBQ toolbox (Draganski et al., 2011; Tabelow et al., 2019). We used maps of magnetization transfer saturation (MT) indicative for tissue myelin (Callaghan et al., 2014; Helms et al., 2008a; Stanisz et al., 1999), transverse relaxation rate ($R2^* = 1/T2^*$) – iron content (Fukunaga et al., 2010; Stüber et al., 2014; Yao et al., 2009), effective longitudinal relaxation rate (R1 = 1/T1) - myelin and iron content (Lutti et al., 2014), and effective proton density (PD^*) - tissue water content (Lin et al., 1997; Watanabe et al., 2019). PD^* maps were normed with a scaling procedure such that mean values in the white matter (WM) agreed with the published level of 69% (Tofts, 2003, chapter 4), which precludes from analyzing PD^* values in the WM. Group-average multi-parameter maps are shown in Fig. 2.

All structural data were processed in the framework of Statistical Parametric Mapping SPM12 (www.fil.ion.ucl.ac.uk/spm; Wellcome Trust Centre for Neuroimaging, London) using customized MATLAB tools (The Mathworks, Sherborn, MA, USA). We performed automated tissue classification using the multi-channel option of SPM12 "unified segmentation" with MT and PD maps and enhanced tissue priors (Lorio et al., 2016) that yielded gray matter (GM), WM, and cerebrospinal fluid (CSF) maps. Total intracranial volumes were calculated as the sum of GM, WM, and CSF volumes.

For analysis within a predefined set of ROIs, we calculated GM regional averages of tissue volume, MT, $R2^*$, PD^*, and R1 using the probabilistic and maximum probability tissue labels derived from the "MICCAI 2012 Grand Challenge and Workshop on Multi-Atlas Labeling" (https://my.vanderbilt.edu/masi/about-us/resources-data/) with 125 cortical and subcortical labels. The labels were spatially registered to individuals' native space using SPM12's diffeomorphic "geodesic shoot" registration (Ashburner and Friston, 2011).

2.3. Data quality assessment

An automated quality assessment procedure was used to flag images potentially deteriorated by intra- and inter-sequence motion artefacts. The latter were estimated from co-registration parameters of MTw and T1w data to the corresponding PDw (threshold = 0.05° for rotations and 3.5 mm for translations). Intra-sequence motion was flagged using the homogeneity (SD/mean) of PDw signal (threshold = 0.1) and from the standard deviation of $R2^*$ in the WM calculated from both T1w and PDw images (threshold = 4.5×10^{-3} ms^{-1}) which correlates to individuals' head motion (Castella et al., 2018). Two experienced neuroscientists visually inspected all data surpassing at least one of the mentioned thresholds. With 94% agreement, they excluded 17 participants' data from the final analysis. Additionally, to exclude images with macroscopic brain abnormalities, we created for each individual a binary mask per tissue class (GM, WM, CSF) with a probability threshold > 0.2 and compared the number of voxels to a canonical group-average tissue map. Among the individuals with fewer voxels in a given tissue class, we identified those surpassing the mean number of missing voxels + 2 SD, excluding 46 additional individuals from the final analysis.

2.4. Clinical and behavioral assessments

Measures of CVRFs collected from questionnaires, blood samples, anthropometric, medication and blood pressure assessments resulted in a comprehensive set indicative of disease history and cardio-vascular risk (Firmann et al., 2008). Aiming at dimensionality reduction for the planned multivariate analyses, we calculated previously established aggregate CVRF scores (aCVRF; Cox et al., 2019) from individuals' assessment of hypertension, diabetes, dyslipidemia, tobacco use, body mass index > 25, waist-to-hip ratio > 0.85 for females or >0.90 for males.

The psychiatric evaluation (Preisig et al., 2009) included the semi-structured Diagnostic Interview for Genetic Studies (DIGS; Nurnberger, 1994). Diagnoses were assigned according to the Diagnostic and Statistical Manual of Mental Disorders (DSM-IV-TR; American Psychiatric Association, 2000). Atypical and melancholic major depressive episodes were diagnosed according to the DSM-IV specifiers. For atypical episodes the presence of mood reactivity as well as two of the following four features were required: i. increased appetite, ii. hypersomnia, iii. leaden paralysis, and iv. interpersonal rejection sensitivity. For melancholic episodes a loss of pleasure or a lack of mood reactivity was required as well as three of the following five symptoms: i. depression regularly worse in the morning, ii. early morning awakening, iii. psychomotor retardation or agitation, iv. decreased appetite, and v. excessive guilt. Participants diagnosed with MDD were classified into one of three categories: i. atypical MDD if they presented atypical but not melancholic episodes, ii. melancholic MDD with melancholic but not atypical episodes, or iii. unspecified MDD if they presented features from neither or both subtypes. The latter category was not analyzed in the present study because of its heterogeneity. Late-life MDD was defined as MDD occurring after the age of 50 years. Bipolar disorder included both types I and II. Anxiety

disorders were defined as presenting at least one of the following characteristics: agoraphobia, generalized anxiety disorder, panic disorder, and social phobia (or social anxiety disorder).

Participants older than 65 years were further tested with a standard cognitive test battery, including the Clinical Dementia Rating (CDR; Morris, 1993), Grober & Buschke Double Memory Test (DMT; Buschke et al., 1997), a verbal fluency task (Cardebat et al., 1990) and the Stroop color test (Stroop, 1935). The verbal fluency score consisted of the number of words correctly produced in a total of 5 min divided between category (semantic) and letter (phonemic) word production segments. A Stroop interference index was calculated by taking the mean time to name incongruent colors (interference) divided by the mean time to name congruent colors (no interference). The Mini-Mental State Examination (MMSE; Folstein et al., 1975) was also assessed in all participants older than 60 years. Aiming to ease interpretation of linear regression analyses, we changed the valence of CDR and Stroop interference scores - in such a way higher scores reflected better performance, similarly to other cognitive scores.

All analyses were done using assessments from the second study follow-up, except for *lifetime* psychiatric measures, which included the whole life period from birth to the second study follow-up. For a comprehensive list of variables see Supplementary Table 1.

2.5. Socio-economic status

We collected information about monthly household gross income, highest educational attainment, and last known occupational position by questionnaire. Monthly income was divided into three categories: up to 4999 CHF (low), 5000-9499 CHF (middle), and more than 9500 CHF (high). Educational attainment was grouped into three levels: mandatory school or apprenticeship (low), high school diploma or upper secondary education (middle), and university degree (high). Occupational position was classified into three levels according to the European Socio-Economic Classification (ESEC) scale (www.iser.essex.ac.uk/archives/esec/user-guide). All three SES measures were included in the extensive association analyses between risk factors and brain structure. Educational level was also used as a covariate of no interest in analyses involving cognitive scores to control for known education effects.

2.6. Statistical analyses

Aiming to exclude potential selection bias, we compared BrainLaus participants to all other CoLaus|PsyCoLaus participants using independent samples t-tests for continuous variables and chi-square tests for categorical variables. For cases of significant difference between samples, we used ordinary least squares (OLS) regression for continuous variables or logistic regression for binary variables to test whether age, sample (BrainLaus participants vs. all other CoLaus|PsyCoLaus participants), or age × sample interaction explained the observed differences. We then calculated correlations between pairs of non-imaging variables using correlation measures adapted to variable types (i.e. the Phi coefficient for dichotomous-dichotomous variables pairs, Point-Biserial correlation for dichotomous-continuous pairs, Pearson's correlation for continuous-continuous pairs, and Spearman's rank correlation for pairs involving ordinal variables with more than two levels). Formally, we tested pairwise associations between each of the eight assessed CVRFs (body mass index (BMI), waist/hip ratio, obesity, hypertension, dyslipidemia, diabetes, smoking, physical activity) and three MDD subtypes (atypical, melancholic, late-life) using logistic regression with age and sex as covariates, and between the eight CVRFs and five cognitive test scores (MMSE, CDR, DMT, verbal fluency, Stroop) using OLS regression with age, sex, and educational level as covariates.

For extensive analyses on all 121 GM and four WM regions, we regressed values in each of the 125 ROIs against each of the 138 non-imaging measures (listed in Supplementary Table 1) using OLS regression, including age, age^2, sex, and total intracranial volume as covariates to the models. We used identical statistical designs for the analysis of GM volume, R1, R2*, MT, and PD*.

For hypothesis-driven analyses, we used an identical statistical design restricted to eight bilateral GM regions and 16 non-imaging measures consisting of the main CVRFs, psychiatric diagnoses, and cognitive test scores. The ROI selection was based on the assumption of their specific involvement in mood disorders (Smagula and Aizenstein, 2016; Ancelin et al., 2019; Wang et al., 2016) and cognitive function (Helie et al., 2013; Tabatabaei-Jafari et al., 2015; Herrmann et al., 2019). The ROIs include the anterior cingulate cortex (ACC), anterior insula, hippocampus, amygdala, caudate, putamen, accumbens, and pallidum, in addition to bilateral cerebral WM (Fig. 4).

To assess the unique contribution of CVRFs and MDD to the variance in brain anatomy features, we performed a Multivariate Analysis of Variance (MANOVA) testing the explanatory power of a combination of MDD diagnosis and CVRFs – hypertension, diabetes, dyslipidemia, obesity, and current tobacco use – on all brain ROI values combined. BMI and waist/hip ratio were not included because of the shared variance with obesity. We tested the main effects of CVRFs and lifetime MDD as well as interactions between CVRFs and MDD subtypes (atypical, melancholic, and late-life MDD). All models were calculated separately for the GM volume, R1, R2*, MT, PD* maps and included age, sex, and TIV as covariates.

We used an identical statistical design for cognitive performance instead of MDD diagnosis. Given that cognitive scores were assessed only in BrainLaus individuals above 65 yo, we abstained from using separate CVRFs as above aiming to reduce the loss of degrees of freedom. Instead, we used the calculated aCVRF score and tested the main effects and interaction effects of aCVRF and cognitive scores, with educational level as additional covariate.

We report results significant at a threshold p-value < 0.05, after applying Bonferroni correction for multiple comparisons and False Discovery Rate (FDR) correction (Benjamini and Hochberg, 1995) where deemed appropriate.

We used Python 3.7 NumPy, Pandas, Statsmodels, and SciPy packages to perform all the statistical analyses.

3. Results

3.1. Sample representativeness validation

The comparison between BrainLaus participants and the rest of the cohort of 3666 with second psychiatric follow-up showed that BrainLaus individuals were younger (mean age difference = 4.0 yrs, $t_{3,664} = 11.5$, $p < 0.001$), though with a small effect size ($d = 0.4$). We observed differences in several socio-demographic, somatic, psychiatric, and cognitive measures between cohorts (see Table 1). Linear regression analyses (Supplementary Tables 2 and 3) showed that all effects were explained by the age difference, and not by the sample (BrainLaus participants vs. all other CoLaus|PsyCoLaus participants) or age × sample interaction.

3.2. Demographic determinants of health

We show that age was associated with an increased waist-to-hip ratio, higher rates of hypertension, dyslipidemia, and diabetes,

Table 1
Comparison between BrainLaus participants and the rest of CoLaus|PsyCoLaus at follow-up 2

	PsyCoLaus (n = 3666)	BrainLaus (n = 1261)	Non-BrainLaus (n = 2405)	T / χ^2	*p* value
Age (mean, SD), yrs	62.9 (10.3)	60.2 (9.2)	64.2 (10.5)	12	<0.001
Sex, % women	55.0	52.6	56.3	4.5	0.03
SES (low/middle/high), %					
Income	26.3/43.8/30.0	22.9/43.1/34.0	28.3/44.2/27.6	17	<0.001
Educational level	50.9/27.2/21.8	48.2/27.7/24.1	52.4/27.0/20.7	7.3	0.03
Last occupational position	42.8/42.3/14.9	43.1/40.9/16.0	42.6/43.1/14.3	1.8	0.4
CVRFs					
BMI (mean, SD), kg/m2	26.4 (4.8)	25.9 (4.5)	26.6 (4.9)	4.1	<0.001
Waist/hip ratio (mean, SD)	0.89 (0.09)	0.88 (0.09)	0.89 (0.09)	3.9	<0.001
Obesity, %	18.8	15.3	20.7	15	<0.001
Hypertension, %	45.0	35.7	50.0	66	<0.001
Dyslipidemia, %	39.8	36.1	41.7	10	0.001
Diabetes, %	10.0	6.2	12.0	29	<0.001
Smoking (current/former/never), %	18.8/39.2/42.0	19.7/36.9/43.4	18.4/40.5/41.1	4.1	0.1
Physical activity (never, 1x/wk, 2x/wk, ≥3x/wk), %	32.3/10.6/56.0/1.1	30.4/12.2/56.4/1.0	33.3/9.7/55.8/1.1	6.8	0.08
Psychiatric diagnoses and scores					
Lifetime MDD, %	48.9	50.6	48.0	2.2	0.1
Atypical MDD, %	17.1	19.8	15.7	9.8	0.002
Melancholic MDD, %	22.9	24.3	22.1	2.2	0.1
Late-life MDD, %	21.5	20.1	22.2	1.9	0.2
Lifetime bipolar disorder, %	2.2	2.8	1.9	2.8	0.1
Lifetime anxiety disorders, %	19.7	21.3	18.8	3.2	0.07
Lifetime GAF score (0-100) (mean, SD)	77.0 (11.5)	77.6 (10.8)	76.7 (11.8)	2.3	0.02
STAI trait score (20-80) (mean, SD)	36.1 (10.4)	36.4 (10.3)	35.9 (10.5)	1.1	0.3
Medication, %					
Antidepressant	11.0	11.6	10.7	0.7	0.4
Tranquilizer	7.7	5.4	9.0	14	<0.001
Cognitive scores (only in ≥ 65 yrs)					
MMSE (0-30) (mean, SD) (in ≥ 60 yrs)	29.1 (1.5)	29.2 (1.4)	29.0 (1.5)	1.5	0.1
CDR score (0/0.5/1), %	48.3/51.0/0.7	50.9/48.8/0.3	47.3/51.9/0.8	2.0	0.4
DMT total free recall (0-64) (mean, SD)	41.3 (9.6)	42.2 (8.7)	41.0 (10.0)	2.0	0.05
Verbal fluency nb. words (mean, SD)	58.1 (16.1)	58.5 (15.7)	57.9 (16.3)	0.6	0.6
Stroop interference index (mean, SD)	2.20 (0.77)	2.18 (0.67)	2.21 (0.80)	0.5	0.6

Comparison between BrainLaus and non-BrainLaus samples by independent samples *t* tests (continuous variables) or chi-square tests (categorical variables).
Key: BMI, body mass index; CDR, Clinical Dementia Rating; DMT, Grober & Buschke Double Memory Test; CVRFs, cardio-vascular risk factors; GAF, Global Assessment of Functioning; MDD, major depressive disorder; MMSE, Mini-Mental State Examination; SES, socioeconomic status; STAI, State-Trait Anxiety Inventory.

and higher occupational position (r ranging 0.09 – 0.37, full correlation matrix in Supplementary Fig. 1). Older age correlated with lower income and education level, lower cognitive scores, lower prevalence of MDD (except late-life MDD) and anxiety disorders (r ranging -0.32 to −0.09). We observed sex differences in several categories (Table 2) – women had a better overall cardio-vascular health, a lower socio-economic status (SES), they were more frequently diagnosed with MDD and anxiety disorders, scored higher on the verbal memory scale and lower on the CDR (|r| ranging 0.08 – 0.58).

3.3. Cardio-vascular risk factors, mood and cognitive performance

Beyond the demographic characteristics, the strongest correlations appeared within each of the categories (SES, CVRFs, psychiatric diagnoses and scores, and cognitive scores). More precisely, there was a large shared variance between measures of SES (r ranging 0.31 – 0.55); CVRFs (|r| ranging 0.09 – 0.75) except smoking; psychometric scores (|r| ranging 0.03 – 0.50); and cognitive scores (|r| ranging 0.08 – 0.44). Additional analyses showed positive correlation between high SES and cardio-vascular health (|r| ranging 0.09 – 0.17), mood (|r| ranging 0.08 – 0.11), and cognitive performance (r ranging 0.14 – 0.31). CVRFs were negatively associated with cognitive outcome (r ranging -0.24 – -0.09, Supplementary Fig. 1b).

There was no significant correlation between CVRFs and psychometric scores when unadjusted for the demographic covariates. After adjustment for age and sex, we observed a significant correlation between atypical MDD, obesity and diabetes (OR of 2.14 and 1.56 respectively, Table 3). The melancholic subtype of MDD correlated with smoking habits (OR = 1.27 for each change in status from never smoked, to former smoker, to current smoker). Late-life MDD showed positive correlation with high BMI (OR = 1.02 for each additional point of BMI), dyslipidemia (OR = 1.25), smoking (OR = 1.30) and low physical activity (OR = 0.86 for each of the four activity frequencies).

In models adjusted for age, sex, and education, all cognitive scores were related to at least one or more CVRFs (Table 4). Waist-to-hip ratio was negatively correlated with all cognitive scores (β = -0.93 for MMSE; 1.07 for CDR; -1.15 for DMT; -1.11 for verbal fluency), except the Stroop test. Diabetes correlated negatively with all cognitive measures (β = -0.21 for MMSE; 0.24 for CDR; -0.26 for DMT; 0.24 for Stroop) except verbal fluency score. The proportion of explained variance in cognitive scores was relatively low (adjusted R^2 ranging from 0.04 for Stroop to 0.15 for DMT).

3.4. Whole-brain regional metrics, cardio-vascular risk and clinical phenotypes

Fig. 3 shows the results of the analyses between regional brain metrics, cardio-vascular risk and clinical phenotypes. Among the 138 somatic and behavioral measures tested, the measures categorized as CVRF showed the strongest correlation with brain anatomy features (Fig. 3a) (threshold at $P_{uncorrected} = 5.83 \times 10^{-7}$ with Bonferroni correction for multiple comparisons). Single variables from other categories – the inflammation marker C-reactive protein, smoking status, the diagnostic entities brief psychotic

Table 2
Sex differences in socioeconomic and clinical characteristics in the BrainLaus sample

	Overall (n = 1261)	Men (n = 598)	Women (n = 663)	T/χ^2	*p* value
Age (mean, SD), yrs	60.2 (9.2)	59.7 (9.2)	60.7 (9.2)	2.0	0.05
SES (low/middle/high), %					
Income	22.9/43.1/34.0	15.8/40.8/43.5	29.5/45.1/25.4	49	<0.001
Educational level	48.2/27.7/24.1	44.3/26.2/29.5	51.7/29.1/19.2	19	<0.001
Last occupational position	43.1/40.9/16.0	35.2/40.0/24.8	50.8/41.9/7.3	61	<0.001
CVRFs					
BMI (mean, SD), kg/m2	25.9 (4.5)	26.6 (3.8)	25.4 (5.0)	4.8	<0.001
Waist/hip ratio (mean, SD)	0.88 (0.09)	0.93 (0.07)	0.83 (0.07)	25	<0.001
Obesity, %	15.3	15.4	15.2	0.0	>0.9
Hypertension, %	35.7	40.6	31.3	11	<0.001
Dyslipidemia, %	36.1	44.9	28.3	37	<0.001
Diabetes, %	6.2	9.4	3.4	18	<0.001
Smoking (current/former/never), %	19.7/36.9/43.4	20.1/41.8/38.1	19.3/32.7/48.0	14	0.001
Physical activity (never, 1x/wk, 2x/wk, ≥3x/wk), %	30.4/12.2/56.4/1.0	31.7/15.9/51.5/0.8	29.2/8.7/60.8/1.2	19	<0.001
Psychiatric diagnoses and scores					
Lifetime MDD, %	50.6	38.6	61.4	64	<0.001
Atypical MDD, %	19.8	11.0	27.8	54	<0.001
Melancholic MDD, %	24.3	16.4	31.5	38	<0.001
Late-life MDD, %	20.1	13.2	26.4	33	<0.001
Lifetime bipolar disorder, %	2.8	2.7	2.9	0.0	>0.9
Lifetime anxiety disorders, %	21.3	17.1	25.2	12	<0.001
Lifetime GAF score (0-100) (mean, SD)	77.6 (10.8)	79.2 (10.2)	76.3 (11.2)	4.8	<0.001
STAI trait score (20-80) (mean, SD)	36.4 (10.3)	34.4 (9.3)	38.0 (10.7)	5.1	<0.001
Medication, %					
Antidepressant	11.6	7.3	15.5	20	<0.001
Tranquilizer	5.4	3.6	7.0	6.6	0.01
Cognitive scores (only in ≥ 65 yrs)					
MMSE (0-30) (mean, SD) (in ≥ 60 yrs)	29.2 (1.4)	29.1 (1.7)	29.2(1.2)	1.5	0.1
CDR score (0/0.5/1), %	50.9/48.8/0.3	42.1/57.1/0.7	57.2/42.8/0.0	8.5	0.01
DMT total free recall (0-64) (mean, SD)	42.2 (8.7)	40.2 (8.8)	43.6 (8.3)	3.6	<0.001
Verbal fluency nb. words (mean, SD)	58.5 (15.7)	58.8 (16.4)	58.3 (15.3)	0.3	0.8
Stroop interference index (mean, SD)	2.18 (0.67)	2.15 (0.58)	2.20 (0.73)	0.8	0.4

Comparison between men and women by independent samples t-tests (continuous variables) or chi-square tests (categorical variables).
Key: BMI, body mass index; CVRFs, cardio-vascular risk factors; CDR, Clinical Dementia Rating; DMT, Grober & Buschke Double Memory Test; GAF, Global Assessment of Functioning; MDD, major depressive disorder; MMSE, Mini-Mental State Examination; SES, socioeconomic status; STAI, State-Trait Anxiety Inventory.

Table 3
Univariate associations between depression subtypes and CVRFs adjusted for age and sex

	Atypical MDD		Melancholic MDD		Late-life MDD	
	OR [95% CI]	***p***	**OR [95% CI]**	***p***	**OR [95% CI]**	***p***
BMI	**1.07 [1.05 – 1.09]**	**<0.001**	1.00 [0.98 – 1.01]	0.8	**1.02 [1.00 – 1.04]**	**0.01**
Waist/hip ratio	**16.3 [4.6 – 57.7]**	**<0.001**	0.83 [0.26 – 2.60]	0.7	3.6 [1.2 – 11.3]	0.03
Obesity	**2.14 [1.73 – 2.65]**	**<0.001**	1.04 [0.85 – 1.29]	0.7	1.25 [1.02 – 1.53]	0.03
Hypertension	1.12 [0.92 – 1.36]	0.3	0.95 [0.80 – 1.14]	0.6	0.96 [0.80 – 1.15]	0.7
Dyslipidemia	1.20 [0.99 – 1.20]	0.06	1.01 [0.85 – 1.20]	0.9	**1.25 [1.05 – 1.48]**	**0.01**
Diabetes	**1.56 [1.13 – 2.15]**	**0.006**	0.91 [0.66 – 1.23]	0.5	1.18 [0.90 – 1.55]	0.2
Smoking	1.13 [1.01 – 1.28]	0.04	**1.27 [1.14 – 1.42]**	**<0.001**	**1.30 [1.16 – 1.45]**	**<0.001**
Physical activity	0.92 [0.84 – 1.01]	0.09	0.98 [0.90 – 1.07]	0.7	**0.86 [0.79 – 0.86]**	**0.001**

Odds ratios (OR) with 95% confidence intervals (CI) and uncorrected *p* values are reported from logistic regression models where MDD measures were individually regressed against CVRFs, including age and sex as covariates.
Significant associations after false discovery rate correction are indicated in bold.
Key: BMI, body mass index; CI, confidence interval; CVRFs, cardio-vascular risk factors; MDD, major depressive disorder; OR, odds ratio.

disorder and schizotypal personality disorder were also correlated with brain anatomy. When considering the less conservative FDR correction (threshold at $P_{uncorrected} = 1.46 \times 10^{-3}$), all categories of somatic, psychiatric, and socio-economic measures showed correlations with brain anatomy mainly in R1, R2*, and MT maps (Fig. 3b, showing respectively 659, 632, and 739 supra-threshold hits for R1, R2*, and MT, while GM volume reached 198 supra-threshold hits).

For the participants older than 65 yrs with cognitive test results and brain imaging (n = 564), the strongest association was with verbal fluency scores (threshold at $P_{uncorrected} = 6.19 \times 10^{-7}$ with Bonferroni correction) (Fig. 3c).

3.5. Whole-brain regional metrics - multi-variate analysis

In a multivariate approach testing the contribution of a combination of CVRFs and MDD lifetime diagnosis to the variance of brain anatomy characteristics (Table 5, Model 1), we observed a significant contribution of hypertension, diabetes, dyslipidemia, obesity, and current smoking status, to brain anatomy across all measured MRI parameters (Wilk's λ ranging 0.35–0.54, $F_{595\text{-}615}$ ranging 1.2–2.1, p-values ranging 4.37×10^{-42}–0.003). In addition to the main effect of CVRFs, there was a main effect of atypical MDD subtype in the MT map ($\lambda = 0.87$, $F_{123} = 1.4$, $p = 0.009$) and a main effect of late-life MDD in R2* ($\lambda = 0.86$, $F_{123} = 1.4$,

Table 4
Univariate associations between cognitive scores and CVRFs after adjusting for age, sex, and educational level

	MMSE		CDR'		DMT		Verbal Fluency		Stroop'	
	ß	*p*	ß	*p*	ß	*p*	ß	*p*	ß	*p*
BMI	-0.01	0.3	-0.001	0.8	-0.003	0.6	**-0.02**	**0.006**	-0.01	0.03
Waist/hip ratio	**-0.93**	**0.003**	**-1.07**	**0.006**	**-1.15**	**0.003**	**-1.11**	**0.005**	-0.71	0.08
Obesity	-0.11	0.06	-0.01	0.9	-0.01	0.9	**-0.20**	**0.005**	-0.11	0.1
Hypertension	-0.05	0.3	-0.02	0.7	-0.13	0.3	-0.13	0.04	-0.06	0.3
Dyslipidemia	-0.04	0.4	-0.01	0.8	-0.01	0.8	-0.05	0.4	**-0.15**	**0.01**
Diabetes	**-0.21**	**0.001**	**-0.24**	**0.003**	**-0.26**	**0.001**	-0.17	0.03	**-0.24**	**0.003**
Smoking	-0.04	0.2	0.003	0.9	0.007	0.9	0.06	0.1	0.008	0.9
Physical activity	**0.08**	**0.001**	0.05	0.07	0.07	0.02	0.07	0.03	**0.08**	**0.009**

Beta coefficients (ß) and uncorrected *p* values are reported from OLS regression models where cognitive scores were individually regressed against CVRFs, including age, sex, and educational level as covariates. CDR and Stroop scores were multiplied by -1 for consistent (higher, better) directionality of scores (CDR' and Stroop').
Significant associations after false discovery rate correction are indicated in bold.
Key: BMI, body mass index; CDR, Clinical Dementia Rating; CVRFs, cardio-vascular risk factors; DMT, Grober & Buschke Double Memory Test; MMSE, Mini-Mental State Examination.

Table 5
MANOVA of R1, R2*, MT, PD*, and volume in brain ROIs, with CVRFs and lifetime diagnosis of MDD as regressors

	R1			R2*			MT			PD*			Volume		
	λ	F (df)	*p*	λ	F (df)	*p*	λ	F (df)	*p*	λ	F (df)	*p*	λ	F (df)	*p*
Model 1															
CVRFs	**0.35**	**2.1 (615)**	**<0.001**	**0.42**	**1.7 (615)**	**<0.001**	**0.42**	**1.7 (615)**	**<0.001**	**0.44**	**1.7 (595)**	**<0.001**	**0.54**	**1.2 (615)**	**0.003**
MDD	0.89	1.1 (123)	0.3	0.91	0.9 (123)	0.7	0.90	1.0 (123)	0.4	0.91	1.0 (119)	0.6	0.89	1.1 (123)	0.3
Model 2															
CVRFs	**0.43**	**1.6 (615)**	**<0.001**	**0.45**	**1.6 (615)**	**<0.001**	**0.46**	**1.5 (615)**	**<0.001**	**0.50**	**1.4 (595)**	**<0.001**	**0.54**	**1.2 (615)**	**0.003**
MDD	0.90	1.0 (123)	0.6	0.90	1.0 (123)	0.5	0.90	0.9 (123)	0.7	0.93	0.7 (119)	>0.9	0.92	0.8 (123)	>0.9
CVRFs × MDD	**0.53**	**1.2 (615)**	**<0.001**	**0.52**	**1.2 (615)**	**<0.001**	0.57	1.1 (615)	0.2	**0.56**	**1.1 (595)**	**0.01**	0.57	1.1 (615)	0.1
Model 3															
CVRFs	**0.39**	**1.9 (615)**	**<0.001**	**0.43**	**1.7 (615)**	**<0.001**	**0.44**	**1.6 (615)**	**<0.001**	**0.47**	**1.5 (595)**	**<0.001**	**0.54**	**1.2 (615)**	**0.007**
Atypical MDD	0.90	1.0 (123)	0.6	0.91	0.9 (123)	0.7	**0.87**	**1.4 (123)**	**0.009**	0.91	0.9 (119)	0.8	0.91	0.9 (123)	0.8
CVRFs × atypical MDD	**0.55**	**1.1 (615)**	**0.02**	**0.53**	**1.2 (615)**	**<0.001**	**0.55**	**1.1 (615)**	**0.02**	0.58	1.1 (595)	0.1	0.59	1.0 (615)	0.6
Model 4															
CVRFs	**0.39**	**1.9 (615)**	**<0.001**	**0.44**	**1.6 (615)**	**<0.001**	**0.45**	**1.6 (615)**	**<0.001**	**0.46**	**1.5 (595)**	**<0.001**	**0.54**	**1.2 (615)**	**0.004**
Melancholic MDD	0.92	0.8 (123)	>0.9	0.92	0.8 (123)	>0.9	0.88	1.2 (123)	0.09	0.92	0.8 (119)	0.9	0.91	0.9 (123)	0.9
CVRFs × melancholic MDD	**0.55**	**1.1 (615)**	**0.01**	0.56	1.1 (615)	0.06	0.56	1.1 (615)	0.07	**0.56**	**1.1 (595)**	**0.02**	0.59	1.0 (615)	0.5
Model 5															
CVRFs	**0.37**	**1.9 (615)**	**<0.001**	**0.44**	**1.6 (615)**	**<0.001**	**0.44**	**1.6 (615)**	**<0.001**	**0.48**	**1.5 (595)**	**<0.001**	**0.55**	**1.2 (615)**	**0.008**
Late-life MDD	0.92	0.8 (123)	>0.9	**0.86**	**1.4 (123)**	**0.003**	0.89	1.1 (123)	0.3	0.90	1.0 (119)	0.5	0.92	0.8 (123)	>0.9
CVRFs × late-life MDD	**0.53**	**1.2 (615)**	**<0.001**	**0.52**	**1.2 (615)**	**<0.001**	**0.54**	**1.2 (615)**	**0.002**	0.57	1.1 (595)	0.06	0.57	1.1 (615)	0.2

Wilk's lambda (λ), F-value, number of degrees of freedom (df), and uncorrected *p* value from Multivariate ANalysis Of VAriance are reported (n = 1234). Each of the five models predicts a linear combination of the brain ROIs (separately for each MRI contrast) from a linear combination of hypertension, diabetes, dyslipidemia, obesity, and current smoking (CVRF) and lifetime MDD diagnoses, with (models 2-5) or without (model 1) interaction between CVRFs and MDD. All models included age, sex, and total intracranial volume as covariates. R1, R2*, MT, and volume included GM and WM regions while PD* included only GM regions.
Significant results after false discovery rate correction are indicated in bold.
Key: CVRFs, cardio-vascular risk factors; GM, gray matter; MDD, major depressive disorder; ROI, region of interest; WM, white matter.

$p = 0.003$). We report interaction between CVRFs and lifetime MDD on R1, R2*, and PD* maps (Model 2, λ ranging 0.52–0.56, $F_{595\text{-}615}$ ranging 1.1–1.2, *p*-values ranging 1.63×10^{-4}–0.01) as well as between CVRFs and atypical MDD (Model 3, R1: $\lambda = 0.55$, $F_{615} = 1.1$, $p = 0.02$; R2*: $\lambda = 0.53$, $F_{615} = 1.2$, $p < 0.001$; MT: $\lambda = 0.55$, $F_{615} = 1.1$, $p = 0.02$), melancholic MDD (Model 4, R1: $\lambda = 0.55$, $F_{615} = 1.1$, $p = 0.01$; PD*: $\lambda = 0.56$, $F_{595} = 1.1$, $p = 0.02$), and late-life MDD (Model 5, R1: $\lambda = 0.53$, $F_{615} = 1.2$, $p < 0.001$; R2*: $\lambda = 0.52$, $F_{615} = 1.2$, $p < 0.001$; MT: $\lambda = 0.54$, $F_{615} = 1.2$, $p = 0.002$).

In the reduced sample of individuals aged ≥ 65 years and tested for cognitive performance (all scores available: n = 306), there was a main effect of the aggregate CVRF score (Table 6, Model 1, R1: $\lambda = 0.44$, $F_{123} = 1.8$, $p < 0.001$; MT: $\lambda = 0.42$, $F_{123} = 2.0$, $p < 0.001$). We did not observe a significant contribution of unique cognitive scores or interaction effects between CVRFs and cognitive performance (Models 1-4).

3.6. Selected region-of-interest analysis

The ROI analysis showed positive correlations between diabetes, smoking status and iron content (R2*) in the basal ganglia (β ranging 0.10 – 0.15; since z-scores were used, one unit increase in β represents one SD increase in MRI measures), and a negative correlation between iron content in the bilateral ACC and the diagnosis of anxiety disorder (β = -0.10 and -0.11). We observed a negative correlation between arterial hypertension and myelin content (MT), particularly in the WM (β = -0.10 and -0.11) contrasted to positive correlation between myelin and obesity (β ranging 0.09 – 0.12). Arterial hypertension, diabetes, obesity, and bipolar disorder in the selected ROIs showed negative correlation with tissue water content (PD*, β ranging -0.12 – -0.08). R1 maps, sensitive to both iron and myelin content, showed positive correlation with diabetes and obesity (β ranging 0.09 – 0.14), and negative correlation with melancholic MDD and anxiety disorders in the hippocampus

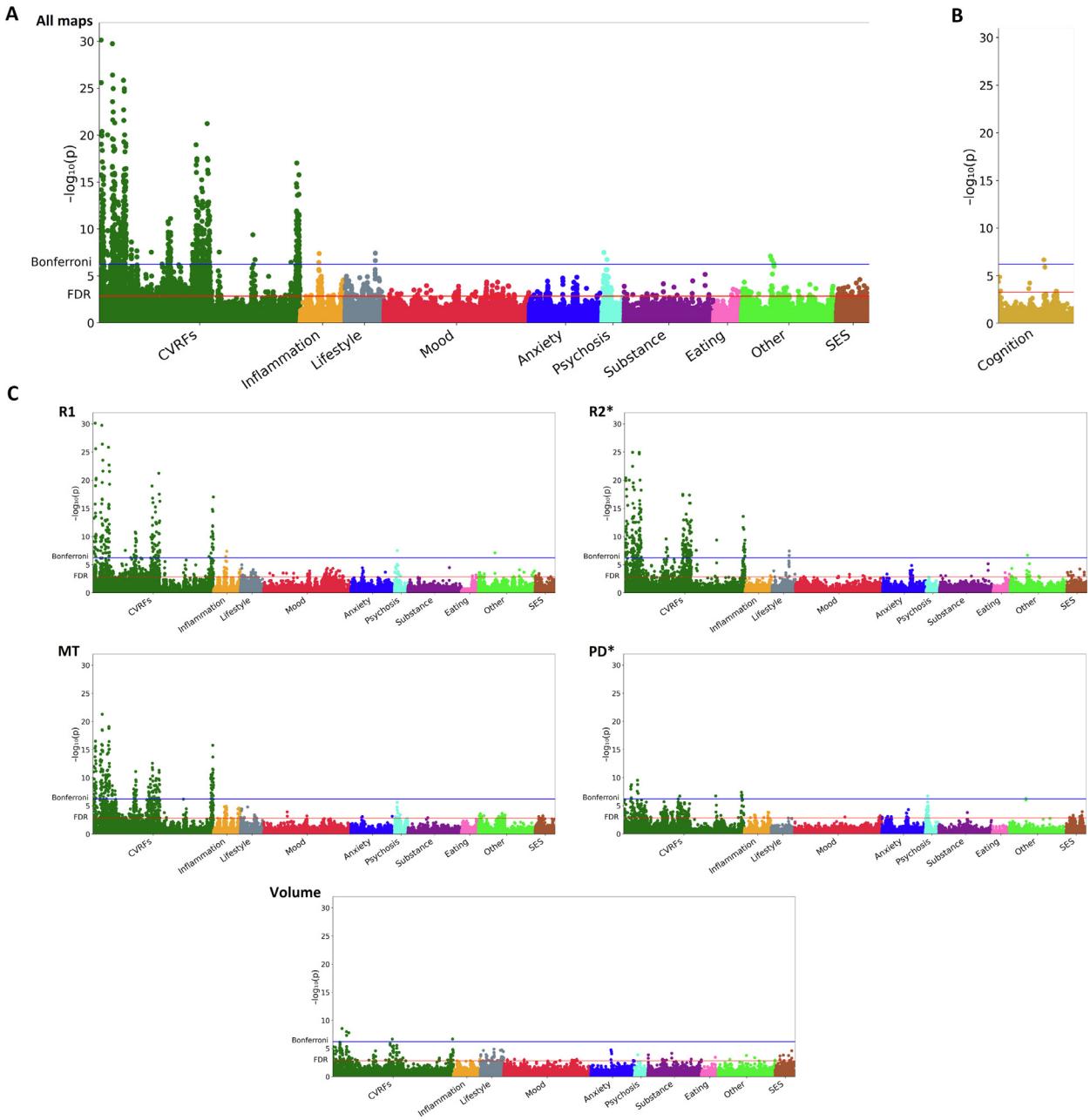

Fig. 3. Manhattan plots relating 621 values from R1, R2*, MT, PD*, and volume maps to 138 non-imaging measures grouped into 10 categories. For each imaging – non-imaging pair, the significance is plotted as -$\log_{10}$(p) of the uncorrected p-value associated with the OLS regression coefficient. Each dot represents one model (i.e. one imaging – non-imaging pair), the 138 non-imaging measures being projected on the x-axis and grouped by categories (see Supplementary Table 1 for a full list of the non-imaging measures). Linear models included sex, age, age^2, and total intracranial volume as covariates. Correction for multiple comparison is indicated as a blue line for Bonferroni correction (threshold at $P_{uncorrected} = 5.83 \times 10^{-7}$) and a red line for FDR correction (threshold at $P_{uncorrected} = 1.46 \times 10^{-3}$) corresponding to the 85,698 tested paired associations. **(A)** All maps are shown together. **(B)** Manhattan plot relating 621 values from R1, R2*, MT, PD*, and volume maps to five cognitive scores, only in participants ≥ 65 years old (n = 564). Bonferroni correction threshold at $P_{uncorrected} = 6.19 \times 10^{-7}$ and FDR threshold at $P_{uncorrected} = 5.42 \times 10^{-4}$ correspond to the 80,730 tested paired associations in this sub-group (621 imaging values × 130 non-imaging variables). **(C)** R1, R2*, MT, PD*, and volume are shown separately. Correction lines show the thresholds corresponding to the total 85,698 tests. Abbreviations: CVRFs = cardio-vascular risk factors; FDR = false discovery rate; OLS = ordinary least squares; SES = socio-economic status. Substance = substance abuse or dependence; Eating = eating disorders; Other = unclassified psychiatric disorders.

(β = -0.09). We report a negative correlation between amygdala volume and diabetes (β ranging -0.09 – -0.05) contrasted to positive correlation with obesity (β ranging 0.05 – 0.13) (Fig. 5). The MMSE, DMT, and verbal fluency scores correlated positively with left amygdala volume (β ranging 0.12 – 0.23). Verbal fluency was also associated with higher PD* in the right putamen (β = 0.18) (Fig. 6).

4. Discussion

Our large-scale monocentric study on mid- and old-age community dwelling adults confirms the wide-ranging association between cardio-vascular risk, cognitive performance, mental health and brain anatomy. We extend the previous findings in the field by analyzing MRI parameters indicative for brain tissue

Table 6
MANOVA of R1, R2*, MT, PD*, and volume in brain ROIs, with aCVRF and cognitive scores as regressors

	R1			R2*			MT			PD*			Volume		
	λ	F (df)	*p*	λ	F (df)	*p*	λ	F (df)	*p*	λ	F (df)	*p*	λ	F (df)	*p*
Model 1															
aCVRF	**0.44**	**1.8 (123)**	**<0.001**	0.51	1.4 (123)	0.03	**0.42**	**2.0 (123)**	**<0.001**	0.56	1.2 (119)	0.1	0.57	1.1 (123)	0.3
DMT	0.54	1.2 (123)	0.1	0.61	0.9 (123)	0.7	0.59	1.0 (123)	0.5	0.61	1.0 (119)	0.5	0.55	1.2 (123)	0.1
VF	0.61	0.9 (123)	0.7	0.54	1.2 (123)	0.1	0.57	1.1 (123)	0.3	0.60	1.0 (119)	0.5	0.57	1.1 (123)	0.3
Stroop	0.52	1.3 (123)	0.05	0.54	1.2 (123)	0.1	0.62	0.9 (123)	0.8	0.58	1.1 (119)	0.3	0.58	1.0 (123)	0.4
Model 2															
aCVRF	**0.43**	**1.9 (123)**	**<0.001**	0.52	1.3 (123)	0.03	**0.43**	**1.9 (123)**	**<0.001**	0.56	1.2 (119)	0.1	0.56	1.1 (123)	0.2
DMT	0.56	1.1 (123)	0.3	0.63	0.8 (123)	0.9	0.64	0.8 (123)	>0.9	0.66	0.8 (119)	>0.9	0.62	0.9 (123)	0.8
aCVRF × DMT	0.51	1.4 (123)	0.03	0.60	1.0 (123)	0.6	0.58	1.0 (123)	0.4	0.62	0.9 (119)	0.6	0.58	1.0 (123)	0.4
Model 3															
aCVRF	**0.45**	**1.7 (123)**	**<0.001**	0.51	1.4 (123)	0.03	**0.42**	**2.0 (123)**	**<0.001**	0.55	1.2 (119)	0.1	0.57	1.1 (123)	0.3
VF	0.61	0.9 (123)	0.7	0.65	0.8 (123)	>0.9	0.59	1.0 (123)	0.5	0.57	1.1 (119)	0.2	0.61	0.9 (123)	0.7
aCVRF × VF	0.56	1.1 (123)	0.3	0.62	0.9 (123)	0.8	0.56	1.1 (123)	0.2	0.57	1.1 (119)	0.2	0.61	0.9 (123)	0.7
Model 4															
aCVRF	**0.45**	**1.8 (123)**	**<0.001**	0.51	1.4 (123)	0.03	**0.43**	**1.9 (123)**	**<0.001**	0.55	1.2 (119)	0.1	0.56	1.1 (123)	0.2
Stroop	0.70	0.6 (123)	>0.9	0.67	0.7 (123)	>0.9	0.59	1.0 (123)	0.5	0.65	0.8 (119)	0.9	0.68	0.7 (123)	>0.9
aCVRF × Stroop	0.62	0.9 (123)	0.7	0.62	0.9 (123)	0.8	0.62	0.9 (123)	0.7	0.63	0.9 (119)	0.8	0.66	0.7 (123)	>0.9

Wilk's lambda (λ), F-value, number of degrees of freedom (df), and uncorrected P-value from Mutlivariate ANalysis Of VAriance are reported (n = 306). Each of the four models predicts a linear combination of the brain ROIs (separately for each MRI contrast) from an aggregate CVRF score and normalised cognitive scores, with (models 2-4) or without (model 1) interaction between aCVRF and cognitive score. All models included age, sex, total intracranial volume, and educational level as covariates. R1, R2*, MT, and volume included GM and WM regions while PD* included only GM regions.
Significant results after false discovery rate correction are indicated in bold.
Key: aCVRF, aggregate cardio-vascular risk factor index; DMT, Grober & Buschke Double Memory Test; GM, gray matter; ROI, region of interest; VF, verbal fluency; WM, white matter.

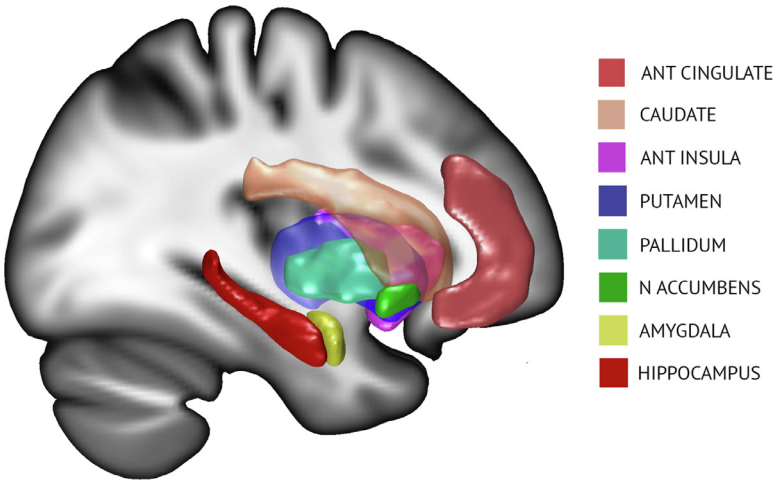

Fig. 4. Selected cortical and subcortical regions-of-interest projected on a standard brain in Montreal Neurological Institute space.

properties – myelin, iron and tissue water, that are complementary to the reporting of regional cortical thickness or volume metrics. Given the constellation of volume and tissue property differences, additionally to the fact that we adjust for the effects of age in all our analyses, we interpret the observed effects as associations between cardio-vascular risk factors and behavioral outcome rather than as effects confounded by ageing.

The complexity of interactions between CVRFs, mood and brain anatomy becomes evident through the observed differential association of CVRFs with the melancholic and atypical MDD subtypes. Our findings support the notion that the two entities differ not only in clinical phenotype characteristics, but also in associated risk factors. Previous findings from prospective cohort studies indicate a temporal sequence between lifestyle factors and late-life depression (Chang et al., 2016; Tanaka et al., 2011), suggesting that targeted intervention on modifiable risk factors could decrease the incidence of late-life MDD. Opposed to their differential CVRFs profile, melancholic and atypical MDD shared the same signature of high iron content in the basal ganglia that could be interpreted in the context of abundant dopamine receptors in subcortical structures and the essential role of iron in dopamine synthesis (Rouault, 2013). The fact that MDD patients, particularly the melancholic and late-life subtypes, have a higher proportion of smokers than the rest, complemented by the observed iron accumulation in smokers' basal ganglia, suggests possible effects of shared variance. At that stage, we can only speculate about the link between basal ganglia dopamine receptors distribution, iron content and tobacco addiction.

A shared feature across all studied psychiatric nosological entities is myelin decrease in the brain's white matter. The decrease was observed for the two metrics indicative for myelin content – the magnetization transfer saturation MT and the longitudinal relaxation rate R1, with the first shown to be the closest to myelin

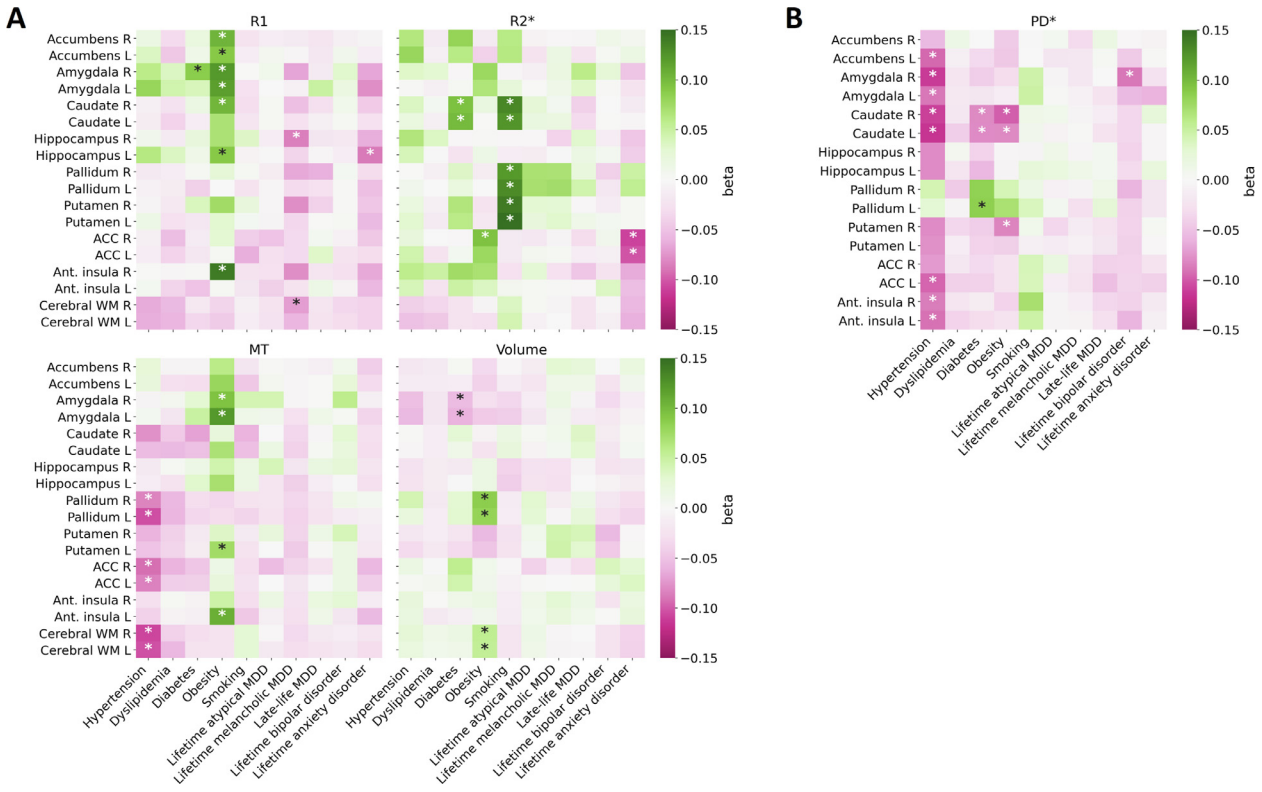

Fig. 5. Beta coefficients from pairwise linear regressions of selected brain regions against cardio-vascular risk factors and psychiatric diagnoses. Local averages of eight GM regions (bilateral) and total cerebral WM (bilateral, when applicable) were individually regressed against main CVRFs and psychiatric diagnoses. To allow comparison between beta coefficients, we normalised brain regional values and non-imaging measures. Linear models included sex, age, age^2, and total intracranial volume as covariates. We show results for **(A)** maps that included cerebral WM and **(B)** the one that did not. Abbreviations: ACC = anterior cingulate cortex; CVRFs = cardio-vascular risk factors; GM = gray matter; MDD = major depressive disorder; WM = white matter. Significant associations after false discovery rate correction are indicated with an asterisk.

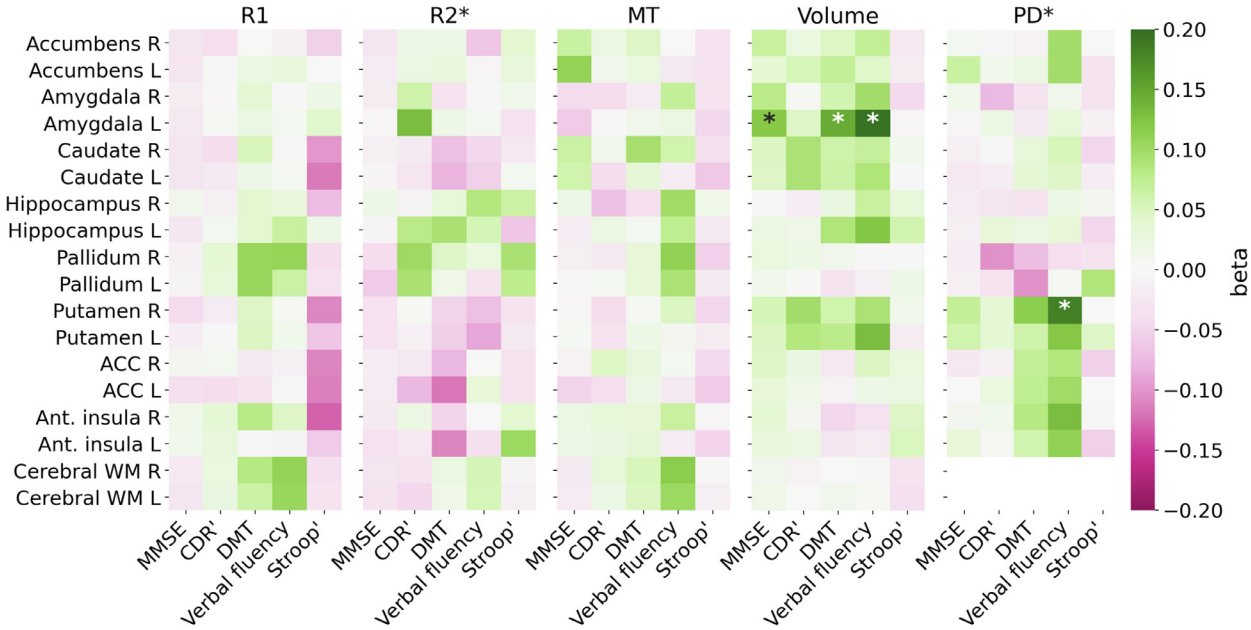

Fig. 6. Beta coefficients from pairwise linear regressions of selected brain regions against cognitive scores. Local averages of eight GM regions (bilateral) and total cerebral WM (bilateral, when applicable) were individually regressed against cognitive scores. To allow comparison between beta coefficients, we normalised brain regional values and cognitive scores, and multiplied CDR and Stroop scores by -1 for consistent (higher = better) directionality of scores (CDR' and Stroop'). Linear models included sex, age, age^2, and total intracranial volume as covariates. Abbreviations: ACC = anterior cingulate cortex; CDR = Clinical Dementia Rating; DMT = Grober & Buschke Double Memory Test; GM = gray matter; MMSE = Mini-Mental State Examination; WM = white matter. Significant associations after false discovery rate correction are indicated with an asterisk.

content metric compared to the majority of existing techniques for direct and indirect measurement of myelin (Mancini et al., 2020). The white matter myelin loss across all CVRFs, particularly in arterial hypertension and in the presence of mood disorders, supports the assumption of "spill-over" effects due to shared variance. This is further enforced by the interaction between myelin content, CVRFs and the atypical/late-life MDD subtypes, but not with the melancholic type – the one that is not necessarily associated with a cardio-vascular risk profile. Despite the differences between our approach to average across the entire white matter volume and the fine-grained tract-based investigation of white matter hyperintensities in a recent study (Dalby et al., 2019), we feel that our results corroborate the reported findings about lack of group differences in abnormal tissue oxygenation in white matter hyperintensities between late-life MDD and individuals without depression. The planned investigation of these effects at the voxel- or tract-based level will help us to determine the topological pattern of changes that should lead to a presumed spatially differential interpretation of our current observations. While CVRFs-related hypoxic tissue injury could underlie the decrease of myelin in late-life depression, astrocyte pathology confined to ventral prefrontal areas could confirm the assumption of myelin reduction in early-life MDD (Rajkowska et al., 2018).

The observed associations between CVRFs and cognitive performance in the sub-group of participants aged 65 and over corroborate published results on the link between obesity, hypercholesterolemia, diabetes, and cognitive decline in older age (Leritz et al., 2011; Marseglia et al., 2019). Similar to previous findings, waist-to-hip ratio proved to be a more sensitive measure than BMI in explaining variability across cognitive scores (Crowe et al., 2018; Liu et al., 2019), particularly for memory and executive functions (Hartanto and Yong, 2018). We note the surprisingly weaker associations between cognitive performance and hippocampus (micro)structure. We explain this by the observed higher predictive value of small-vessel disease-related anatomy changes compared with baseline differences (Moon et al., 2017), additionally to the reduced statistical power of this subgroup analysis when compared to the whole BrainLaus cohort ($n = 306$ vs. 1234). Alternatively, the absence of significant effects may be due to the larger shared variance with individuals' education attainment level, which was included as a covariate in the model. The positive association between left amygdala volume, MMSE, verbal memory and verbal fluency scores may reflect cognitive decline in preclinical Alzheimer's disease due to local beta-amyloid and tau pathology as recently reported (Betthauser et al., 2020), which is further supported by the left-sided predominance of our language system-related findings. Verbal memory and verbal fluency scores also showed a trend for negative correlation with iron content. The latter can be interpreted in the context of the "free-radical induced energetic decline in senescence" model that suggests iron-related oxidative stress as a mediator of ageing effects on brain anatomy and cognitive function (Daugherty and Raz, 2015; Raz and Daugherty, 2018).

Given the exploratory character of our analysis of cardio-vascular, inflammatory, lifestyle factors, mood, anxiety and cognition, we adjusted for the confounding effects of sex and age, whilst acknowledging potential interaction effects. The observed lower CVRFs and higher verbal memory scores, paralleled by higher depression and anxiety morbidity in women are consistent with previous reports (Altemus et al., 2014; Peters et al., 2019) and suggest differential mechanisms of association between modifiable risk factors and cognitive and mental health in men and women. We carefully adjusted for the confounding effects of SES, which was positively correlated with cardio-vascular and mental health. Individuals with low SES have a higher incidence of psychiatric disorders (Zimmerman and Katon, 2005) and cardio-vascular disease (Elo et al., 2014; Kamphuis et al., 2012; Stringhini et al., 2017) suggesting that SES at least partly mediates the association between CVRFs and mental disorders. It is of note that we observed a relatively high lifetime prevalence of MDD in our sample – 50.6 % when considering all MDD subtypes – compared to meta-analytic reports of 10-21% lifetime MDD prevalence in European countries (Lim et al., 2018; Gutiérrez-Rojas et al., 2020). As discussed previously (Vandeleur et al., 2017), one possible explanation is that the CoLaus|PsyCoLaus sample was recruited from an urban population known to be more susceptible to psychiatric disorders (Peen et al., 2007). Another line of argumentation is defined by the semi-structured character of the Diagnostic Interview for Genetic Studies (DIGS) instrument used for psychiatric assessment in CoLaus|PsyCoLaus that results in more frequent positive diagnosis than fully-structured interview methods (Eaton et al., 2000). The latter type of methods may under-estimate the prevalence of depression in the community (Kruijshaar et al., 2005).

The novelty of our study is mainly in providing complementary information about brain-behavior relationship by analyzing MRI parameters derived from established biophysical models and allowing for a straightforward neuro-biological interpretation (Weiskopf et al., 2015). Our findings of reduced longitudinal relaxation time R1 fit well in the presumed mechanism of CVRFs-related decrease in interstitial fluid mobility and water content that predates or co-occurs with demyelination and gliosis captured by the MT saturation (Maniega et al., 2015). Given that R1 is a weighted average of the free and bound water phases, empirical research showed that a large part of the R1 variance was shared with MT and $R2^*$ (Callaghan et al., 2015). We interpret the residual correlations between R1 and CVRFs after regressing out the effects of MT and $R2^*$, as an independent contribution of the total water content to brain microstructure (Supplementary Fig. 2). Contrary to our expectations of a negative impact of obesity on white matter's myelin, we observed a positive correlation that merits further investigation, particularly in the context of ApoE allelic variants as demonstrated recently (Mole et al., 2020).

There are some limitations in our study that should be acknowledged. Given the focus on urban population, the generalizability of our results is uncertain. The cross-sectional data not only limits the interpretations to correlation analysis findings, but it also hampers assessing the impact of inter-individual differences on brain and behavior that, particularly in the cognitive domain, will increase with advancing age (Nyberg et al., 2020). By adopting a region-of-interest approach as in the UK Biobank (Miller et al., 2016), we refrained from a whole-brain analysis as reported previously (Taubert et al., 2020), which can be seen as a potential weak point of the current report. The shared variance between age, lifetime factors and the outcome variables in our study – cognitive performance and mood – pose a challenge for a straightforward interpretation of the obtained results. Attempts to formally test these relationships using structural equation modelling or similar techniques for mediation analysis do not resolve the issue of complex interdependencies that are potentially addressable by longitudinal studies (e.g. Veldsman et al., 2020). Alternatively, the authors provide a highly selective set of lifetime variables that help avoiding shared variance and the dilemma of interpretability but omit a range of factors that could explain additional variance (e.g. Opel et al., 2020).

In summary, the presented results on brain anatomy patterns that link cardio-vascular risk factors, mood and cognition showed main effects and complex interactions in the context of ageing. The fact that CVRFs correlated with both brain tissue microstructure and volume differences underscores the complementary character of MRI parameter mapping that is closer to the underlying neu-

robiological mechanisms and reduces the probability of spurious morphometric findings.

Credit Author Statement

Conception and design of the study: OT and BD.

Acquisition and analysis of data: OT, LLK, GDD, AL, MK, SS, PMV, PV, GW, MP, FK, BD.

Drafting a significant portion of the manuscript or figures: OT, MK, SS, PMV, PV, GW, MP, FK, BD

Disclosure statement

The authors declare that there is no conflict of interest related to this work.

Acknowledgments

We would like to thank all participants in the BrainLaus study. This work was supported by the Leenaards Foundation with a Translational Medicine prize (to SS, MK and BD). BD is supported by the Swiss National Science Foundation (project grant numbers 32003B_135679, 32003B_159780, 324730_192755, and CRSK-3_190185). AL is supported by the Swiss National Science Foundation (project grant number 320030_184784) and the ROGER DE SPOELBERCH foundation. GW is supported by the Swiss National Science Foundation (project grant number 32003B_173092). FK received funds from H2020-EU Morphemic project (grant agreement ID: 871643). LREN is very grateful to the ROGER DE SPOELBERCH and Partridge Foundations for their generous financial support. The CoLaus|PsyCoLaus study was and is supported by research grants from GlaxoSmithKline; the Faculty of Biology and Medicine of Lausanne; and the Swiss National Science Foundation (grants numbers 3200B0_105993, 3200B0_118308, 33CSCO_122661, 33CS30_139468, and 33CS30_14840). The graphical abstract was created with BioRender.com.

Supplementary materials

Supplementary material associated with this article can be found, in the online version, at doi:10.1016/j.neurobiolaging.2021.02.002.

References

Åberg, M.A.I., Nyberg, J., Torén, K., Sörberg, A., Kuhn, H.G., Waern, M., 2014. Cardiovascular fitness in early adulthood and future suicidal behaviour in men followed for up to 42 years. Psychol. Med 44 (4), 779–788. doi:10.1017/S0033291713001207.

Åberg, M.A.I., Waern, M., Nyberg, J., Pedersen, N.L., Bergh, Y., Åberg, N.D., Nilsson, M., Kuhn, H.G., Torén, K., 2012. Cardiovascular fitness in males at age 18 and risk of serious depression in adulthood: Swedish prospective population-based study. Br. J. Psychiatry 201 (5), 352–359. doi:10.1192/bjp.bp.111.103416.

Altemus, M., Sarvaiya, N., Neill Epperson, C., 2014. Sex differences in anxiety and depression clinical perspectives. Front. Neuroendocrinol. 35 (3), 320–330. doi:10.1016/j.yfrne.2014.05.004.

American Psychiatric Association, 2000. Diagnostic and Statistical Manual of Mental Disorders, Fourth Edition American Psychiatric Association, Arlington, VA Text Revision (DSM-IV-TR). 4th ed..

Ancelin, M.-L., Carrière, I., Artero, S., Maller, J., Meslin, C., Ritchie, K., Ryan, J., Chaudieu, I., 2019. Lifetime major depression and grey-matter volume. J. Psychiatry Neurosci. 44 (1), 45–53. doi:10.1503/jpn.180026.

Ashburner, J., Friston, K.J., 2011. Diffeomorphic registration using geodesic shooting and Gauss-Newton optimisation. Neuroimage 55 (3), 954–967. doi:10.1016/j.neuroimage.2010.12.049.

Baghai, T.C., Varallo-Bedarida, G., Born, C., Häfner, S., Schüle, C., Eser, D., Rupprecht, R., Bondy, B., von Schacky, C., 2011. Major depressive disorder is associated with cardiovascular risk factors and low omega-3 index. J. Clin. Psychiatry 72 (09), 1242–1247. doi:10.4088/JCP.09m05895blu.

Benjamini, Y., Hochberg, Y., 1995. Controlling the false discovery rate: a practical and powerful approach to multiple testing. J. R. Stat. Soc. Ser. B Methodol. 57 (1), 289–300. doi:10.2307/2346101.

van den Berg, K.S., Wiersema, C., Hegeman, J.M., van den Brink, R.H.S., Rhebergen, D., Marijnissen, R.M., Oude Voshaar, RC, 2019. Clinical characteristics of late-life depression predicting mortality. Aging Ment. Health 1–8. doi:10.1080/13607863.2019.1699900.

Betthauser, T.J., Koscik, R.L., Jonaitis, E.M., Allison, S.L., Cody, K.A., Erickson, C.M., Rowley, H.A., Stone, C.K., Mueller, K.D., Clark, L.R., et al., 2020. Amyloid and tau imaging biomarkers explain cognitive decline from late middle-age. Brain 143 (1), 320–335. doi:10.1093/brain/awz378.

Buschke, H., Sliwinski, M.J., Kuslansky, G., Lipton, R.B., 1997. Diagnosis of early dementia by the double memory test: encoding specificity improves diagnostic sensitivity and specificity. Neurology 48 (4), 989–996. doi:10.1212/WNL.48.4.989.

Callaghan, M.F., Freund, P., Draganski, B., Anderson, E., Cappelletti, M., Chowdhury, R., Diedrichsen, J., FitzGerald, T.H.B., Smittenaar, P., Helms, G., et al., 2014. Widespread age-related differences in the human brain microstructure revealed by quantitative magnetic resonance imaging. Neurobiol. Aging 35 (8), 1862–1872. doi:10.1016/j.neurobiolaging.2014.02.008.

Callaghan, M.F., Helms, G., Lutti, A., Mohammadi, S., Weiskopf, N., 2015. A general linear relaxometry model of R 1 using imaging data: General Linear Relaxometry Model of R1. Magn. Reson. Med. 73 (3), 1309–1314. doi:10.1002/mrm.25210.

Cardebat, D., Doyon, B., Puel, M., Goulet, P., Joanette, Y., 1990. Formal and semantic lexical evocation in normal subjects. Performance and dynamics of production as a function of sex, age and educational level. Acta Neurol. Belg. 90 (4), 207–217.

Castella, R., Arn, L., Dupuis, E., Callaghan, M.F., Draganski, B., Lutti, A., 2018. Controlling motion artefact levels in MR images by suspending data acquisition during periods of head motion: Castella et al. Magn. Reson. Med. 80 (6), 2415–2426. doi:10.1002/mrm.27214.

Chang, S.C., Pan, A., Kawachi, I., Okereke, O.I., 2016. Risk factors for late-life depression: a prospective cohort study among older women. Prev. Med. 91, 144–151. doi:10.1016/j.ypmed.2016.08.014.

Cox, S.R., Lyall, D.M., Ritchie, S.J., Bastin, M.E., Harris, M.A., Buchanan, C.R., Fawns-Ritchie, C., Barbu, M.C., de Nooij, L., Reus, L.M., et al., 2019. Associations between vascular risk factors and brain MRI indices in UK Biobank. Eur. Heart J. 40 (28), 2290–2300. doi:10.1093/eurheartj/ehz100.

Crowe, M., Dávila-Roman, A., Barba, C., Downer, B., Andel, R., 2018. Waist-hip ratio, body mass index, and cognitive decline in older puerto ricans. Innov. Aging 2 (Suppl 1), 255. doi:10.1093/geroni/igy023.950.

Dalby, R.B., Eskildsen, S.F., Videbech, P., Frandsen, J., Mouridsen, K., Sørensen, L., Jeppesen, P., Bek, T., Rosenberg, R., Østergaard, L., 2019. Oxygenation differs among white matter hyperintensities, intersected fiber tracts and unaffected white matter. Brain Commun. 1 (1), fcz033. doi:10.1093/braincomms/fcz033.

Daugherty, A.M., Raz, N., 2015. Appraising the role of iron in brain aging and cognition: promises and limitations of MRI methods. Neuropsychol. Rev. 25 (3), 272–287. doi:10.1007/s11065-015-9292-y.

Deckers, K., Schievink, S.H.J., Rodriquez, M.M.F., Van Oostenbrugge, R.J., Van Boxtel, M.P.J., Verhey, F.R.J., Köhler, S., 2017. Coronary heart disease and risk for cognitive impairment or dementia: systematic review and meta-analysis. PLoS One 12 (9), e0184244. doi:10.1371/journal.pone.0184244.

Dhar, A.K., Barton, D.A., 2016. Depression and the link with cardiovascular disease. Front. Psychiatry 7, 33. doi:10.3389/fpsyt.2016.00033.

Draganski, B., Ashburner, J., Hutton, C., Kherif, F., Frackowiak, R.S.J., Helms, G., Weiskopf, N., 2011. Regional specificity of MRI contrast parameter changes in normal ageing revealed by voxel-based quantification (VBQ). Neuroimage 55 (4), 1423–1434. doi:10.1016/j.neuroimage.2011.01.052.

Eaton, W.W., Neufeld, K., Chen, L.-S., Cai, G., 2000. A comparison of self-report and clinical diagnostic interviews for depression: diagnostic interview schedule and schedules for clinical assessment in neuropsychiatry in the baltimore epidemiologic catchment area follow-up. Arch. Gen. Psychiatry 57 (3), 217. doi:10.1001/archpsyc.57.3.217.

Elo, I.T., Martikainen, P., Myrskylä, M., 2014. Socioeconomic status across the life course and all-cause and cause-specific mortality in Finland. Soc. Sci. Med. 119, 198–206. doi:10.1016/j.socscimed.2013.11.037.

Fiedorowicz, J.G., 2014. Depression and cardiovascular disease: an update on how course of illness may influence risk. Curr. Psychiatry Rep. 16 (10), 492. doi:10.1007/s11920-014-0492-6.

Firmann, M., Mayor, V., Vidal, P.M., Bochud, M., Pécoud, A., Hayoz, D., Paccaud, F., Preisig, M., Song, K.S., Yuan, X., et al., 2008. The CoLaus study: a population-based study to investigate the epidemiology and genetic determinants of cardiovascular risk factors and metabolic syndrome. BMC Cardiovasc. Disord. 8, 6. doi:10.1186/1471-2261-8-6.

Folstein, M.F., Folstein, S.E., McHugh, P.R., 1975. Mini-mental state. J. Psychiatr. Res. 12 (3), 189–198. doi:10.1016/0022-3956(75)90026-6.

Foreman, K.J., Marquez, N., Dolgert, A., Fukutaki, K., Fullman, N., McGaughey, M., Pletcher, M.A., Smith, A.E., Tang, K., Yuan, C.W., et al., 2018. Forecasting life expectancy, years of life lost, and all-cause and cause-specific mortality for 250 causes of death: reference and alternative scenarios for 2016–40 for 195 countries and territories. Lancet 392 (10159), 2052–2090. doi:10.1016/S0140-6736(18)31694-5.

Fukunaga, M., Li, T.-Q., van Gelderen, P., de Zwart, J.A., Shmueli, K., Yao, B., Lee, J., Maric, D., Aronova, M.A., Zhang, G., et al., 2010. Layer-specific variation of iron

content in cerebral cortex as a source of MRI contrast. Proc. Natl. Acad. Sci. 107 (8), 3834–3839. doi:10.1073/pnas.0911177107.
Geerlings, M.I., Gerritsen, L., 2017. Late-life depression, hippocampal volumes, and hypothalamic-pituitary-adrenal axis regulation: a systematic review and meta-analysis. Biol. Psychiatry 82 (5), 339–350. doi:10.1016/j.biopsych.2016.12.032.
Gutiérrez-Rojas, L., Porras-Segovia, A., Dunne, H., Andrade-González, N., Cervilla, J.A., 2020. Prevalence and correlates of major depressive disorder: a systematic review. Braz. J. Psychiatry 42 (6), 657–672. doi:10.1590/1516-4446-2020-0650.
Hamer, M., Batty, G.D., 2019. Association of body mass index and waist-to-hip ratio with brain structure: UK Biobank study. Neurology 92 (6), e594–e600. doi:10.1212/WNL.0000000000006879.
Hartanto, A., Yong, J.C., 2018. Measurement matters: Higher waist-to-hip ratio but not body mass index is associated with deficits in executive functions and episodic memory. PeerJ 6, e5624. doi:10.7717/peerj.5624.
Helie, S., Chakravarthy, S., Moustafa, A.A., 2013. Exploring the cognitive and motor functions of the basal ganglia: an integrative review of computational cognitive neuroscience models. Front. Comput. Neurosci. 7, 174. doi:10.3389/fncom.2013.00174.
Helms, G., Dathe, H., Dechent, P., 2008. Quantitative FLASH MRI at 3T using a rational approximation of the Ernst equation. Magn. Reson. Med. 59 (3), 667–672. doi:10.1002/mrm.21542.
Helms, G., Dathe, H., Kallenberg, K., Dechent, P., 2008. High-resolution maps of magnetization transfer with inherent correction for RF inhomogeneity and T 1 relaxation obtained from 3D FLASH MRI. Magn. Reson. Med. 60 (6), 1396–1407. doi:10.1002/mrm.21732.
Herrmann, F.R., Rodriguez, C., Haller, S., Garibotto, V., Montandon, M.-L., Giannakopoulos, P., 2019. Gray matter densities in limbic areas and APOE4 independently predict cognitive decline in normal brain aging. Front. Aging Neurosci. 11, 157. doi:10.3389/fnagi.2019.00157.
Jani, B.D., Cavanagh, J., Barry, S.J., Der, G., Sattar, N., Mair, F.S., 2014. Revisiting the J shaped curve, exploring the association between cardiovascular risk factors and concurrent depressive symptoms in patients with cardiometabolic disease: findings from a large cross-sectional study. BMC Cardiovasc. Disord. 14, 139. doi:10.1186/1471-2261-14-139.
Kamphuis, C.B., Turrell, G., Giskes, K., MacKenbach, J.P., Van Lenthe, F.J., 2012. Socioeconomic inequalities in cardiovascular mortality and the role of childhood socioeconomic conditions and adulthood risk factors: a prospective cohort study with 17-years of follow up. BMC Public Health 12, 1045. doi:10.1186/1471-2458-12-1045.
Killin, L.O.J., Starr, J.M., Shiue, I.J., Russ, T.C., 2016. Environmental risk factors for dementia: a systematic review. BMC Geriatr. 16 (1), 175. doi:10.1186/s12877-016-0342-y.
Kivipelto, M., Mangialasche, F., Ngandu, T., 2018. Lifestyle interventions to prevent cognitive impairment, dementia and Alzheimer disease. Nat. Rev. Neurol. 14 (11), 653–666. doi:10.1038/s41582-018-0070-3.
Kontis, V., Bennett, J.E., Mathers, C.D., Li, G., Foreman, K., Ezzati, M., 2017. Future life expectancy in 35 industrialised countries: projections with a Bayesian model ensemble. Lancet 389 (10076), 1323–1335. doi:10.1016/S0140-6736(16)32381-9.
Kruijshaar, M.E., Barendregt, J., Vos, T., de Graaf, R., Spijker, J., Andrews, G., 2005. Lifetime prevalence estimates of major depression: an indirect estimation method and a quantification of recall bias. Eur. J. Epidemiol. 20 (1), 103–111. doi:10.1007/s10654-004-1009-0.
Leritz, E.C., McGlinchey, R.E., Kellison, I., Rudolph, J.L., Milberg, W.P., 2011. Cardiovascular disease risk factors and cognition in the elderly. Curr. Cardiovasc. Risk Rep. 5 (5), 407–412. doi:10.1007/s12170-011-0189-x.
Lim, G.Y., Tam, W.W., Lu, Y., Ho, C.S., Zhang, M.W., Ho, R.C., 2018. Prevalence of depression in the community from 30 countries between 1994 and 2014. Sci. Rep. 8 (1), 2861. doi:10.1038/s41598-018-21243-x.
Lin, W., Paczynski, R.P., Venkatesan, R., He, Y.Y., Powers, W.J., Hsu, C.Y., Haacke, E.M., 1997. Quantitative regional brain water measurement with magnetic resonance imaging in a focal ischemia model. Magn. Reson. Med. 38 (2), 303–310. doi:10.1002/mrm.1910380221.
Liu, Z., Yang, H., Chen, S., Cai, J., Huang, Z., 2019. The association between body mass index, waist circumference, waist-hip ratio and cognitive disorder in older adults. J Public Health (Oxf) 41 (2), 305–312. doi:10.1093/pubmed/fdy121.
Lorio, S., Fresard, S., Adaszewski, S., Kherif, F., Chowdhury, R., Frackowiak, R.S., Ashburner, J., Helms, G., Weiskopf, N., Lutti, A., et al., 2016. New tissue priors for improved automated classification of subcortical brain structures on MRI. Neuroimage 130, 157–166. doi:10.1016/j.neuroimage.2016.01.062.
Lorio, S., Kherif, F., Ruef, A., Melie-Garcia, L., Frackowiak, R., Ashburner, J., Helms, G., Lutti, A., Draganski, B., 2016. Neurobiological origin of spurious brain morphological changes: a quantitative MRI study. Hum. Brain Mapp. 37 (5), 1801–1815. doi:10.1002/hbm.23137.
Lutti, A., Dick, F., Sereno, M.I., Weiskopf, N., 2014. Using high-resolution quantitative mapping of R1 as an index of cortical myelination. Neuroimage (93 Pt 2) 176–188. doi:10.1016/j.neuroimage.2013.06.005.
Lutti, A., Hutton, C., Finsterbusch, J., Helms, G., Weiskopf, N., 2010. Optimization and validation of methods for mapping of the radiofrequency transmit field at 3T. Magn. Reson. Med. 64 (1), 229–238. doi:10.1002/mrm.22421.
Lutti, A., Stadler, J., Josephs, O., Windischberger, C., Speck, O., Bernarding, J., Hutton, C., Weiskopf, N., 2012. Robust and fast whole brain mapping of the RF transmit field B1 at 7T. Zhan W, editor. PLoS One 7 (3), e32379. doi:10.1371/journal.pone.0032379.
Mancini, M., Karakuzu, A., Cohen-Adad, J., Cercignani, M., Nichols, T.E., Stikov, N., 2020. An interactive meta-analysis of MRI biomarkers of myelin. Elife 9, e61523. doi:10.7554/eLife.61523.
Maniega, S.M., Valdés Hernández, M.C., Clayden, J.D., Royle, N.A., Murray, C., Morris, Z., Aribisala, B.S., Gow, A.J., Starr, J.M., Bastin, M.E., et al., 2015. White matter hyperintensities and normal-appearing white matter integrity in the aging brain. Neurobiol. Aging 36 (2), 909–918. doi:10.1016/j.neurobiolaging.2014.07.048.
Marseglia, A., Fratiglioni, L., Kalpouzos, G., Wang, R., Bäckman, L., Xu, W., 2019. Prediabetes and diabetes accelerate cognitive decline and predict microvascular lesions: a population-based cohort study. Alzheimers Dement. 15 (1), 25–33. doi:10.1016/j.jalz.2018.06.3060.
Miller, K.L., Alfaro-Almagro, F., Bangerter, N.K., Thomas, D.L., Yacoub, E., Xu, J., Bartsch, A.J., Jbabdi, S., Sotiropoulos, S.N., Andersson, J.L.R., et al., 2016. Multimodal population brain imaging in the UK Biobank prospective epidemiological study. Nat. Neurosci. 19 (11), 1523–1536. doi:10.1038/nn.4393.
Mole, J.P., Fasano, F., Evans, J., Sims, R., Hamilton, D.A., Kidd, E., Metzler-Baddeley, C., 2020. Genetic risk of dementia modifies obesity effects on white matter myelin in cognitively healthy adults. Neurobiol. Aging 94, 298–310. doi:10.1016/j.neurobiolaging.2020.06.014.
Moon, S.Y., de, S.o.u.t.o., Barreto, P., Chupin, M., Mangin, J.F., Bouyahia, A., Fillon, L., Andrieu, S., Vellas, B., 2017. Associations between white matter hyperintensities and cognitive decline over three years in non-dementia older adults with memory complaints. J. Neurol. Sci. 379, 266–270. doi:10.1016/j.jns.2017.06.031.
Morris, J.C., 1993. The Clinical Dementia Rating (CDR): current version and scoring rules. Neurology 43 (11), 2412. doi:10.1212/WNL.43.11.2412-a.
Natu, V.S., Gomez, J., Barnett, M., Jeska, B., Kirilina, E., Jaeger, C., Zhen, Z., Cox, S., Weiner, K.S., Weiskopf, N., et al., 2019. Apparent thinning of human visual cortex during childhood is associated with myelination. Proc. Natl. Acad. Sci. U S A 116 (41), 20750–20759. doi:10.1073/pnas.1904931116.
Nurnberger, J.I., 1994. Diagnostic interview for genetic studies: rationale, unique features, and training. Arch. Gen. Psychiatry 51 (11), 849. doi:10.1001/archpsyc.1994.03950110009002.
Nyberg, L., Boraxbekk, C.-J., Sörman, D.E., Hansson, P., Herlitz, A., Kauppi, K., Ljungberg, J.K., Lövheim, H., Lundquist, A., Adolfsson, A.N., et al., 2020. Biological and environmental predictors of heterogeneity in neurocognitive ageing. Ageing Res. Rev. 64, 101184. doi:10.1016/j.arr.2020.101184.
Opel, N., Thalamuthu, A., Milaneschi, Y., Grotegerd, D., Flint, C., Leenings, R., Goltermann, J., Richter, M., Hahn, T., Woditsch, G., et al., 2020. Brain structural abnormalities in obesity: relation to age, genetic risk, and common psychiatric disorders. Mol Psychiatry https://doi.org/10.1038/s41380-020-0774-9. In press.
Peen, J., Dekker, J., Schoevers, R.A., Have, M.ten, de Graaf, R., Beekman, A.T., 2007. Is the prevalence of psychiatric disorders associated with urbanization? Soc. Psychiatry Psychiatr. Epidemiol. 42 (12), 984–989. doi:10.1007/s00127-007-0256-2.
Peters, S.A.E., Muntner, P., Woodward, M., 2019. Sex differences in the prevalence of, and trends in, cardiovascular risk factors, treatment, and control in the United States, 2001 to 2016. Circulation 139 (8), 1025–1035. doi:10.1161/CIRCULATIONAHA.118.035550.
Preisig, M., Waeber, G., Vollenweider, P., Bovet, P., Rothen, S., Vandeleur, C., Guex, P., Middleton, L., Waterworth, D., Mooser, V., et al., 2009. The PsyCoLaus study: methodology and characteristics of the sample of a population-based survey on psychiatric disorders and their association with genetic and cardiovascular risk factors. BMC Psychiatry 9, 9. doi:10.1186/1471-244X-9-9.
Prins, N.D., Scheltens, P., 2015. White matter hyperintensities, cognitive impairment and dementia: an update. Nat. Rev. Neurol. 11 (3), 157–165. doi:10.1038/nrneurol.2015.10.
Rajkowska, G., Legutko, B., Moulana, M., Syed, M., Romero, D.G., Stockmeier, C.A., Miguel-Hidalgo, J.J., 2018. Astrocyte pathology in the ventral prefrontal white matter in depression. J. Psychiatr. Res. 102, 150–158. doi:10.1016/j.jpsychires.2018.04.005.
Raz, N., Daugherty, A.M., 2018. Pathways to brain aging and their modifiers: Free-Radical-Induced Energetic and Neural Decline in Senescence (FRIENDS) model—a mini-review. Gerontology 64 (1), 49–57. doi:10.1159/000479508.
Rouault, T.A., 2013. Iron metabolism in the CNS: implications for neurodegenerative diseases. Nat. Rev. Neurosci. 14 (8), 551–564. doi:10.1038/nrn3453.
Ruan, Q., D'Onofrio, G., Sancarlo, D., Bao, Z., Greco, A., Yu, Z., 2016. Potential neuroimaging biomarkers of pathologic brain changes in Mild Cognitive Impairment and Alzheimer's disease: a systematic review. BMC Geriatr. 16, 104. doi:10.1186/s12877-016-0281-7.
Rubin, R.R., Gaussoin, S.A., Peyrot, M., Dilillo, V., Miller, K., Wadden, T.A., West, D.S., Wing, R.R., Knowler, W.C., 2010. Cardiovascular disease risk factors, depression symptoms and antidepressant medicine use in the Look AHEAD (Action for Health in Diabetes) clinical trial of weight loss in diabetes. Diabetologia 53 (8), 1581–1589. doi:10.1007/s00125-010-1765-1.
Shafto, M.A., Tyler, L.K., Dixon, M., Taylor, J.R., Rowe, J.B., Cusack, R., Calder, A.J., Marslen-Wilson, W.D., Duncan, J., Dalgleish, T., et al., 2014. The Cambridge Centre for Ageing and Neuroscience (Cam-CAN) study protocol: a cross-sectional, lifespan, multidisciplinary examination of healthy cognitive ageing. BMC Neurol. 14, 204. doi:10.1186/s12883-014-0204-1.
Smagula, S.F., Aizenstein, H.J., 2016. Brain structural connectivity in late-life major depressive disorder. Biol. Psychiatry Cogn. Neurosci. Neuroimaging 1 (3), 271–277. doi:10.1016/j.bpsc.2015.11.005.
Stanisz, G.J., Kecojevic, A., Bronskill, M.J., Henkelman, R.M., 1999. Characterizing white matter with magnetization transfer andT2. Magn. Reson. Med. 42

(6), 1128–1136. doi:10.1002/(sici)1522-2594(199912)42:6<1128::aid-mrm18>3.0.co;2-9.
Stringhini, S., Carmeli, C., Jokela, M., Avendaño, M., Muennig, P., Guida, F., Ricceri, F., d'Errico, A., Barros, H., Bochud, M., et al., 2017. Socioeconomic status and the 25 × 25 risk factors as determinants of premature mortality: a multicohort study and meta-analysis of 1•7 million men and women. Lancet 389 (10075), 1229–1237. doi:10.1016/S0140-6736(16)32380-7.
Stroop, J.R., 1935. Studies of interference in serial verbal reactions. J. Exp. Psychol. 18 (6), 643–662. doi:10.1037/h0054651.
Stüber, C., Morawski, M., Schäfer, A., Labadie, C., Wähnert, M., Leuze, C., Streicher, M., Barapatre, N., Reimann, K., Geyer, S., et al., 2014. Myelin and iron concentration in the human brain: a quantitative study of MRI contrast. Neuroimage 93, 95–106. doi:10.1016/j.neuroimage.2014.02.026.
Sudlow, C., Gallacher, J., Allen, N., Beral, V., Burton, P., Danesh, J., Downey, P., Elliott, P., Green, J., Landray, M., et al., 2015. UK Biobank: an open access resource for identifying the causes of a wide range of complex diseases of middle and old age. PLoS Med. 12 (3), e1001779. doi:10.1371/journal.pmed.1001779.
Tabatabaei-Jafari, H., Shaw, M.E., Cherbuin, N., 2015. Cerebral atrophy in mild cognitive impairment: a systematic review with meta-analysis. Alzheimers Dement. Diagn. Assess. Dis. Monit. 1 (4), 487–504. doi:10.1016/j.dadm.2015.11.002.
Tabelow, K., Balteau, E., Ashburner, J., Callaghan, M.F., Draganski, B., Helms, G., Kherif, F., Leutritz, T., Lutti, A., Phillips, C., et al., 2019. hMRI—a toolbox for quantitative MRI in neuroscience and clinical research. Neuroimage 194, 191–210. doi:10.1016/j.neuroimage.2019.01.029.
Takeda, J.R.T., Matos, T.M., Souza-Talarico, J.N.de, 2017. Cardiovascular risk factors and cognitive performance in aging. Dement. Neuropsychol. 11 (4), 442–448. doi:10.1590/1980-57642016dn11-040015.
Tanaka, H., Sasazawa, Y., Suzuki, S., Nakazawa, M., Koyama, H., 2011. Health status and lifestyle factors as predictors of depression in middle-aged and elderly Japanese adults: a seven-year follow-up of the Komo-Ise cohort study. BMC Psychiatry 11, 20. doi:10.1186/1471-244X-11-20.
Taubert, M., Roggenhofer, E., Melie-Garcia, L., Muller, S., Lehmann, N., Preisig, M., Vollenweider, P., Marques-Vidal, P., Lutti, A., Kherif, F., et al., 2020. Converging patterns of aging-associated brain volume loss and tissue microstructure differences. Neurobiol. Aging 88, 108–118. doi:10.1016/j.neurobiolaging.2020.01.006.
Tofts, P. (Ed.), 2003. Quantitative MRI of the Brain John Wiley & Sons, Ltd., Chichester, UK doi:10.1002/0470869526.
Vaccarino, V., Badimon, L., Bremner, J.D., Cenko, E., Cubedo, J., Dorobantu, M., Duncker, D.J., Koller, A., Manfrini, O., Milicic, D., et al., 2020. Depression and coronary heart disease: 2018 position paper of the ESC working group on coronary pathophysiology and microcirculation. Eur. Heart J. 41 (17), 1687–1696. doi:10.1093/eurheartj/ehy913.
Van der Kooy, K., van Hout, H., Marwijk, H., Marten, H., Stehouwer, C., Beekman, A., 2007. Depression and the risk for cardiovascular diseases: systematic review and meta analysis. Int. J. Geriatr. Psychiatry 22 (7), 613–626. doi:10.1002/gps.1723.
Vandeleur, C.L., Fassassi, S., Castelao, E., Glaus, J., Strippoli, M.-P.F., Lasserre, A.M., Rudaz, D., Gebreab, S., Pistis, G., Aubry, J.-M., et al., 2017. Prevalence and correlates of DSM-5 major depressive and related disorders in the community. Psychiatry Res. 250, 50–58. doi:10.1016/j.psychres.2017.01.060.
Veldsman, M., Tai, X.-Y., Nichols, T., Smith, S., Peixoto, J., Manohar, S., Husain, M., 2020. Cerebrovascular risk factors impact frontoparietal network integrity and executive function in healthy ageing. Nat. Commun. 11 (1), 4340. doi:10.1038/s41467-020-18201-5.
Wang, M., Norman, J.E., Srinivasan, V.J., Rutledge, J.C., 2016. Metabolic, inflammatory, and microvascular determinants of white matter disease and cognitive decline. Am. J. Neurodegener. Dis. 5 (5), 171–177.
Watanabe, T., Wang, X., Tan, Z., Frahm, J., 2019. Magnetic resonance imaging of brain cell water. Sci. Rep. 9, 5084. doi:10.1038/s41598-019-41587-2.
Weiskopf, N., Mohammadi, S., Lutti, A., Callaghan, M.F., 2015. Advances in MRI-based computational neuroanatomy: from morphometry to in-vivo histology. Curr. Opin. Neurol. 28 (4), 313–322. doi:10.1097/WCO.0000000000000222.
Weiskopf, N., Suckling, J., Williams, G., Correia, M.M.M., Inkster, B., Tait, R., Ooi, C., Bullmore, T.E.T., Lutti, A., 2013. Quantitative multi-parameter mapping of R1, PD*, MT, and R2* at 3T: a multi-center validation. Front. Neurosci. 7, 95. doi:10.3389/fnins.2013.00095.
Woelfer, M., Kasties, V., Kahlfuss, S., Walter, M., 2019. The role of depressive subtypes within the neuroinflammation hypothesis of major depressive disorder. Neuroscience 403, 93–110. doi:10.1016/j.neuroscience.2018.03.034.
Yao, B., Li, T., Gelderen, P., Shmueli, K., Dezwart, J., Duyn, J., 2009. Susceptibility contrast in high field MRI of human brain as a function of tissue iron content. Neuroimage 44 (4), 1259–1266. doi:10.1016/j.neuroimage.2008.10.029.
Zimmerman, F.J., Katon, W., 2005. Socioeconomic status, depression disparities, and financial strain: what lies behind the income-depression relationship? Health Econ. 14 (12), 1197–1215. doi:10.1002/hec.1011.